INNOVATIVE AND CONVENTIONAL MODELLING FOR AVIAN ACOUSTIC AND FIRE SEVERITY ANALYSES

by

Yi-Chin Tseng

B.Sc., National Taiwan University, 2017

A THESIS SUBMITTED IN PARTIAL FULFILLMENT OF

THE REQUIREMENTS FOR THE DEGREE OF

MASTER OF SCIENCE

in

THE FACULTY OF GRADUATE AND POSTDOCTORAL STUDIES

(Forestry)

THE UNIVERSITY OF BRITISH COLUMBIA

(Vancouver)

November 2019

The following individuals certify that they have read, and recommend to the Faculty of Graduate and Postdoctoral Studies for acceptance, a thesis entitled:

Innovative and conventional modelling for avian acoustic and fire severity analyses

submitted by Yi-Chin Tseng in partial fulfillment of the requirements for

the degree of Master of Science

in Forestry

Examining Committee:

Bianca N.I. Eskelson (Forest Resources Management)
Supervisor

Kathy Martin (Forest and Conservation Sciences)
Supervisory Committee Member

Nicholas C. Coops (Forest Resources Management)
Supervisory Committee Member

Darren Irwin (Zoology)
Additional Examiner

Abstract

Data science, the principles that support extracting knowledge from data, has become increasingly important in natural resources management. This thesis applied both machine learning (innovative modelling) and statistics (conventional modelling) to address two ecological questions.

In **Chapter 2**, **Automatic bird sound detection: logistic regression based acoustic occupancy model**, logistic models and convolutional neural networks were applied to predict bird presence/absence in audio recordings, in order to improve efficiency in analyzing large audio datasets. The acoustic recordings came from a bird sound detection challenge organized by the Institute of Electrical and Electronics Engineers (IEEE) and covered bird songs and calls in a wide range of environments along with the presence of noise. Based on leave-one-out cross-validation, the final logistic model resulted in an overall accuracy of 75% with a false negative rate of 16%. Compared with a convolutional neural network (CNN) model using the same dataset, the logistic model was about seven times faster in terms of processing time. This bird sound detection model using sound frequency percentiles in a logistic model opens up promising approaches to aid in automatic, accurate, and efficient analysis of large audio datasets for monitoring wildlife communities.

In **Chapter 3**, **Previous fire severity enhances reburn severity: a case study in interior British Columbia, Canada**, an ordinal logistic model was applied to investigate how previous fires influenced the reburn severity in interior British Columbia, Canada, in order to determine the driver of reburn severity. Previous fires affect rates of fuel consumption and accumulation, thus influencing the probability and severity of subsequent fires. In this study, forest stand structural change due to the first fire (in 2009 or 2010), such as changes in basal area and trees per hectare, were used to model the severity of the reburn in 2017. The ordinal model indicated a positive relationship between fire severities in the Riske Creek area. Specifically, fires in the Riske Creek area might not be able to limit the probability or severity of a reburn after seven or eight years.

Lay Summary

This thesis applied modelling methods to answer two ecological questions. First, a bird sound detection model was developed to distinguish audio recordings including bird sound from recordings with noises. The final model achieved a high overall accuracy (75%) and reduced required processing resources compared to the state-of-the art models, convolutional neural network models. This study opens up promising approaches to aid in automatic, accurate, and efficient analysis of large audio datasets for monitoring wildlife communities. Second, an ordinal model was developed to investigate how previous fires influence reburn severity. The final model indicated that higher severity in a previous fire was related to high reburn severity in the Riske Creek area in interior British Columbia, Canada. This result indicated that previous severe fires might not be able to limit the probability or severity of a reburn after seven or eight years of a fire in the Riske Creek area.

.

Preface

The audio recordings dataset used in Chapter 2 came from a Bird Audio Detection challenge of the Institute of Electrical and Electronics Engineers (IEEE). Dr. Valerie LeMay assisted with identifying the research questions and developing the methods. All the data organization, exploration, and analysis were performed by me under supervision of Dr. Valerie LeMay and Dr. Bianca Eskelson. The chapter was written by me with input from Drs. Valerie LeMay, Bianca Eskelson, Kathy Martin, and Nicholas Coops.

The field data used in Chapter 3 were provided by Dr. Kathy Martin from her project "Nestweb: A study of cavity nesting communities in Riske and Knife Creeks". The 2018 post-fire field data were collected by me and Alice Miao as field assistant. Drs. Bianca Eskelson, Kathy Martin, and Vincente Monleon from the United States Department of Agriculture Forest Service assisted with the development of the 2018 post-fire field protocol. All the field data entry was performed by me and Alice Miao. Dr. Bianca and Dr. Kathy Martin assisted with identifying the research questions and developing analysis methods. All the data organization, exploration, and analysis were performed by me under supervision of Dr. Bianca Eskelson. The chapter was written by me with input from Drs. Bianca Eskelson, Kathy Martin, and Nicholas Coops.

The thesis is the original, unpublished work of the author, Yi-Chin Tseng. All figures, tables, and writing are my own work. Chapter 2 will be submitted for publication upon acceptance of the thesis, with Drs. Bianca Eskelson, Kathy Martin, and Valerie LeMay as co-authors.

Table of Contents

Abstract .... **iii**

Lay Summary .... **v**

Preface .... **vi**

Table of Contents .... **vii**

List of Tables .... **ix**

List of Figures .... **xi**

List of Abbreviations .... **xiv**

Acknowledgements .... **xv**

Dedication .... **xvii**

Chapter 1: Introduction **1**

Chapter 2: Automatic bird sound detection: logistic regression based acoustic occupancy model **4**

2.1 Introduction 4

2.2 Methods 7

2.3 Results 16

2.4 Discussion 26

2.5 Conclusions 31

Chapter 3: Previous fire severity enhances reburn severity: a case study in interior British Columbia, Canada **32**

3.1 Introduction 32

3.2 Methods 34

3.3 Results 44

3.4 Discussion 50

3.5 Conclusions 56

Chapter 4: Conclusion 57

4.1 Overall conclusions and future work 57

4.2 Limitations to the studies 58

4.3 Data science in action 59

References 61

Appendix: Additional figures and tables for Chapter 3 72

List of Tables

Table 2-1 Number of audio recordings by data source and bird presence/absence. 8

Table 2-2 Logistic detection model comparison for selecting base model (upper part) and conducting variable selection based on the selected base model (lower part). 20

Table 2-3 Processing times and model performance comparison between the logistic model and the CNN. Processing times were tested on a computer with an Intel Core i7-4790 CPU operating at 3.6 GHz. 25

Table 3-1 Tree basal area per hectare (BA), percent BA by species, and mean, standard deviation (SD), and maximum (max) diameter at breast height (DBH) prior to the first fire: 2008 measurement for RC, RL, RP and 2010 for MG, SW. Species code: trembling aspen (AT), lodgepole pine (PL), Douglas-fir (FD), spruce sp. (Sx). Numbers in bold font indicate the dominant tree species on each site. 37

Table 3-2 Forest patch type of each site, number of total plots, plots that were experienced by mountain pine beetle (MPB), and plots that were salvaged due to the mountain pine beetle outbreak or the grassland restoration (managed pre-1st fire). 39

Table 3-3 Soil fire severity classification key for the reburn severity. 41

Table 3-4 t-test for comparing the mean, and Levene's test for comparing the variance of pre-first fire stand structure in two forest patch types. The p-values in bold font indicate the pairs with significant differences (α=0.05).. 45

Table 3-5 Model parameters and corresponding p-values. Variables were identified as statistically significant (p-value ≤ 0.05) and as providing suggestive but inconclusive evidence in the model (0.05 < p-value ≤0.1) (Ramsey and Schafer 2013). 49

Table 3-6 Confusion matrix to compare predicted and observed reburn severity. Elements in the confusion matrix represented the number of plots in each combination of predicted and observed reburn severity. Refer to Table 3-3 for details of the reburn severity definition. 49

Table A-1 Basal area per hectare, species composition, tree density, and DBH distribution by site in 1998. Abbreviations: DBH: diameter at the breast height; SD: standard deviation. 72

Table A-2 Basal area per hectare, species composition, tree density, and DBH distribution by sites post first fire. Post first fire: 2010 measurement for RC, RL, RP and 2011 for MG, SW. Abbreviation: DBH: diameter at the breast height; SD: standard deviation................................ 73

Table A-3 Basal area per hectare, species composition, tree density, and DBH distribution by sites post-reburn (2018). Abbreviation: DBH: diameter at the breast height; SD: standard deviation.. 74

Table A-4 Predicted probabilities (P) for each reburn severity categories, predicted reburn severity category, and observed reburn severity category. 76

List of Figures

Figure 2-1 Process of extracting sound frequency percentiles from a recording. (a) Spectrogram of a ten-second long recording. (b) Dominant sound frequencies selected from each of the sound frames in the spectrogram. (c) Empirical cumulative distribution of dominant sound frequencies. The 99^{th} percentile was marked by dashed lines for demonstration. 10

Figure 2-2 The complete convolutional neural network (CNN) model architecture used in this study. The numbers indicate the dimension of the object. The input layer of the model is the spectrogram of the recording and the output is the predicted probability of the presence of bird sounds. 15

Figure 2-3 Illustration of audio recordings with and without bird sounds, specifically: (a) spectrograms of a recording with bird sounds (top), and a recording with human speech and traffic noise (bottom); and (b) associated empirical cumulative distributions of dominant sound frequencies. 17

Figure 2-4 Sound frequency percentiles versus mean dominant sound frequencies with 99% confidence interval marked as horizontal error bars. Audio recordings were grouped by with (orange) and without (green). 18

Figure 2-5 The distributions of predicted probabilities for recordings with (orange) versus without (green) bird sounds. The left and right side of the boxes are the first quantile (Q1) and the third quantile (Q3) of the predicted probabilities, respectively. The recordings with bird sounds had a higher median predicted probability (0.72) than that of recordings without bird sounds (0.20). 22

Figure 2-6 Observed presence proportions versus predicted probabilities for 20 equal-interval predicted probability groups (blue bubbles). The size of the bubbles represents the number of recordings in each group. The fitted line (solid blue line) is shown along with a 95% confidence band (gray area), compared with a 1:1 correspondence (dashed red line). 23

Figure 2-7 (a) Overall accuracy (blue), (b) false negative rate (green), and false positive rate (red) across a gradient of cut-off probabilities. 24

Figure 3-1 Burn area of the three wildfires and location of the five study sites: Military Gate (MG), Rock Complex (RC), Rock Lake (RL), Rock Pine (RP), and Solitary Woods (SW). Each of the five sites was composed of a cluster of plots (black dots). 36

Figure 3-2 Examples of soil fire severity categories a) no evidence of a recent fire, b) surface organic cover ≥ 85 %, c) surface organic cover ≥ 40 % and < 85 %, and d) surface organic cover < 40 %, respectively (Refer to Table 3-3 for details). 41

Figure 3-3 (a) Live and (b) standing dead tree density (trees per hectare, TPH) of the three dominant species in the study area. TPH was influenced by mountain pine beetle outbreak, post mountain pine beetle salvage logging, grassland restoration, and fires in 2009/2010 (highlighted in yellow). No measurements were available between 2012 and 2017. Therefore, the period is represented with dashed lines. 46

Figure 3-4 Spatial distribution of post-fire management and the reburn severity categories in each of the five sites. Refer to Table 3-3 for the soil fire severity classification key. 47

Figure A-1 Percentage of dead pines in each plot before the first fire. Salvage logging occurred in some of the plots in 2007 and 2008. 75

Figure A-2 Post-fire logging in 2011 left large size logging debris on site, which might resulte in severe reburn in 2017. Photo taken by Yi-Chin Tseng for plot MGB3 in 2018 June. 79

Figure A-3 Post-fire logging in 2011 left large size logging debris on site, which might resulte in severe reburn in 2017. Photo taken by Yi-Chin Tseng for plot MGB4 in 2018 June. 80

List of Abbreviations

AIC – Akaike information criterion

ARU – autonomous recording unit

AUC – area under a ROC curve

BA – basal area per hectare

BC – British Columbia

CNN – convolutional neural network

DBH – diameter at breast height

IDF – interior Douglas-fir biogeoclimate zone

IEEE – Institute of Electrical and Electronics Engineers

MG – Military Gate

MPB – mountain pine beetle

RC – Rock Complex

RL – Rock Lake

RP – Rock Pine

ROC – relative operating characteristic

SD – standard deviation

SW – Solitary Woods

TPH – trees per hectare

WAV – waveform audio file format

Acknowledgements

I express my gratitude to my academic supervisor, Dr. Bianca N.I. Eskelson, for making this thesis possible. Her supervision and guidance have made me become a stronger person. Great thanks to Dr. Kathy Martin, who took me to the field sites in Williams Lake, taught me how to drive field vehicles, and helped me network with people in the ornithology field. I admire her great enthusiasm in science and her intelligence. Special thanks to Dr. Nicholas Coops – although our meetings never went more than 10 minutes, his insights to scientific research and his positive energy have guided me through the process of my study. I offer my enduring gratitude to Dr. Valerie LeMay, for the patience and confidence she has shown in me. I am sincerely grateful for our numerous discussion sessions covering many different topics.

Thanks to Dr. Darren Irwin and Ildiko Szabo. The term I took the ornithology course and volunteered in the Beaty Biodiversity Museum was the most amazing time during my study.

Thanks to Alice Miao for our wonderful two months fieldwork in Williams Lake. I will forever miss the time we had with the big red truck, the mosquitos, and the windstorm that we experienced together. Thanks to Shelley, Jared (Fletcher family), Sandy, Ken, John, Judy, Richard, and Faye for giving me such wonderful memory in Williams Lake and making this city like home for me.

I am fortunate to work in a friendly environment in the Biometrics lab: special thanks to Stella B. Acquah, who provided me the strongest emotional support, Nguyet-Anh Nguyen (Moon), who provided me delicious food when I needed rescues, and Woongsoon Jang, who helped me polish my writing skills through numerous discussions. Thanks to my friends, Edith Li, Sam Herniman, Zoe Davis, and Samual Grubinger, for always being there to support me.

Special thanks to Peter Ward, who taught me so much about bird sound recording. I am truly fortunate to know him and to learn from his amazing personality.

Although my study often kept me busy and required to stay far away from my home country, my family and friends in Taiwan have always been supportive, inspiring, and a source of happiness. Special thanks to my mom for her generous emotional support during these 2.5 years. I would not have been able to accomplish this without her.

Dedication

To our splendid Nature.

Chapter 1: Introduction

Data science, the principles that support extracting knowledge from data, has changed the world we are living in today (Dhar 2012). Jordan (2019) argued that data science is an amalgamation of statistics (conventional modelling) and machine learning (innovative modelling), two fields that are closely related in terms of their nature of discovering patterns in data, but distinct in their primary goals of application (Dhar 2012). Statistics has a great focus on the interpretability of a model, aiming to derive causal inference and inference to a population using experimental and observational studies, respectively (Ramsey and Schafer 2013). In contrast, machine learning finds the underlying patterns of data, with a strong emphasis on prediction instead of interpretation (Dhar 2012). Nowadays we are seeing widespread application of data science to fill the gap between data generation and data understanding (van der Aalst 2016). Current scientific research across all disciplines requires a certain level of understanding in statistics and/or machine learning, in order to draw inferences or make predictions (Dhar 2012).

Skills in statistics and/or machine learning in the field of natural resources management have become increasingly important given the great quantity of available data (Song et al. 2018). Collecting data across large spatio-temporal scales has become relatively easy with advanced technology such as unmanned aerial vehicles, camera trapping, and autonomous recording units (Pimm et al. 2015). Efforts have been made to synthesize collected data and, accordingly, numerous open source databases are available such as the EarthExplorer for Landsat imagery (https://earthexplorer.usgs.gov/), Monitoring Trends in Burn Severity database (https://www.mtbs.gov/), Global Biodiversity Information Facility (https://www.gbif.org/), National Ecological Observatory Network (https://www.neonscience.org/), iNaturalist (https://www.inaturalist.org/), Xeno-Canto (https://www.xeno-canto.org/), and eBird (https://ebird.org/home). These databases provide opportunities for large scale research in natural resources management, such as wildfire monitoring, landscape management, biological monitoring, and animal movement (Pimm et al. 2015). As a result, we are seeing a change in the natural sciences from how to collect enough data to how to appropriately analyze data, understand the limitations of diverse methods, and turn data into insights (Arts et al. 2015).

Successful stories about applying data science in the field of natural resources management emerged over the past few years: the collective behaviour in birds was studied using quantitative computer vision analysis (Procaccini et al. 2011); illegal logging in rainforests was monitored by cellphone-based devices using harmonics detection in acoustical analysis (Upton et al. 2015); endangered and rare species were surveyed by camera traps and individuals were detected using automatic recognition analysis (O'Connell et al. 2011, Tabak et al. 2019); and avian populations were examined with autonomous recording units using acoustic analysis (Shonfield and Bayne 2017). In the information age that we are living in today, creativity and strong analytical skills are key for successful research (Arts et al. 2015).

In this thesis, two ecological questions in the field of natural resources management were answered using statistics and machine learning approaches. In particular, the strength of data science being able to make predictions and draw inferences from data were demonstrated. In **Chapter 2**, **Automatic bird sound detection: logistic regression based acoustic occupancy model**, logistic models and convolutional neural networks were applied to predict bird presence/absence in audio recordings, in order to improve the efficiency in analyzing large audio datasets. Specific objectives of this chapter were: 1) to test the effectiveness of using sound frequency percentiles in a logistic model to predict the presence of bird sounds in audio recordings, 2) to compare the performance of this approach to results from a CNN approach, and 3) to provide an open source algorithm to implement both detection models. This study provides an efficient and accurate algorithm for detecting birds from audio recordings that could potentially be used in a wide variety of environments. In **Chapter 3**, **Previous fire severity enhances reburn severity: a case study in interior British Columbia, Canada**, an ordinal logistic model was applied to investigate how previous fire influence the reburn severity in the Riske Creek area in interior British Columbia, Canada, in order to determine the driver of reburn severity. Here a statistical model was developed as an explanatory model to relate the stand structure change due to the first fire to the reburn severity. Specific objectives of this chapter were: 1) to describe and compare the pre-first fire stand structure, including species composition, tree density, and basal area, between continuous and fragmented forest patches, and 2) to identify whether the severity of the first fire, which was represented by basal area and density metrics, enhances or limits the reburn severity.

Chapter 2: Automatic bird sound detection: logistic regression based acoustic occupancy model

2.1 Introduction

The use of autonomous recording units (ARUs) for avian biodiversity assessments and community assembly investigations across landscapes has become increasingly popular in recent years (Sueur et al. 2014, Shonfield and Bayne 2017). ARUs enabled scheduled and continuous collection of soundscapes. Given the reliability of aural detection by field observers during point count surveys (Simons et al. 2007), acoustic surveys with ARUs have been used for deriving ecological indices such as species occupancy (Lambert and McDonald 2014, Sovern et al. 2014, Drake et al. 2016), and abundance (Hedley et al. 2017). Large-scale monitoring with ARUs has been widely applied to assess avian community composition (Klingbeil and Willig 2015), monitor endangered birds (Garnett et al. 2011), and conduct bird counting (Rosenstock et al. 2002).

Despite increasing interest in using ARUs, analyzing audio recordings continues to be a challenge given the terabytes of data generated by large-scale monitoring projects (Joly et al. 2019). Accordingly, commercial and open source software have been developed to assist bird species identification from audio recordings (Shonfield and Bayne 2017), including Song Scope (Wildlife Acoustic, Maynard, Massachusetts, USA), Kaleidoscope Pro (Wildlife Acoustic, Maynard, Massachusetts, USA), Raven Pro (Cornell Laboratory of Ornithology, Ithaca, New

York, USA), Sound Analysis Pro (Tchernichovski et al. 2000), and the R package ‘monitor’ (Hafner and Katz 2017). However, using species identification software generally requires substantial computational processing time and memory resources. One way to minimize the processing time and memory resources is to filter the recording periods without bird sounds before using the software (Stowell et al. 2016). A pre-filtering step is especially useful for audio recordings collected with low bird sound activity, such as acoustic recordings collected for nocturnal birds (Rognan et al. 2012). Specifically, employing an automatic detection algorithm as a pre-filtering step can greatly increase the efficiency of audio analysis.

Convolutional neural network (CNN) is the state-of-the art model form that has been widely applied for detecting sound events in audio recordings, and has demonstrated high accuracy in distinguishing recordings with versus without bird sounds (Adavanne et al. 2017, Cakir et al. 2017, Kong et al. 2017, Pellegrini 2017). A CNN contains a series of convolutional layers that include filters to be applied on the input image (i.e., spectrograms from audio recordings in this case), and enable a model to recognize underlying relationships in a set of images. However, training a CNN model generally requires considerable computational resources. Further, a CNN typically contains thousands of parameters in order to define kernels in convolutions layers, making the interpretation of model parameters a hard task.

Logistic models (i.e., generalized linear models using a logit link and a binomial distribution) are another model form that often be used for predicting the existence of wildlife given their simplicity, effectiveness, and relative ease of interpretation (Mladenoff et al.1999). A previous study showed that logistic detection models can achieve similar accuracy as neural network detection models but can greatly reduce the computational resources and enable drawing statistical inferences (Ayer et al. 2010). Logistic prediction models can relate a binary response variable, bird presence or absence in the case of bird sound detection, with predictor variables extracted from audio recordings. Several low-level descriptive parametric representations (i.e., dimension reduction approach) have been proven to be simple and powerful predictor variables for vocalization detection. For example, peak spectral components of recordings have been used to detect flight calls (Tanttu et al. 2006); highest frequency and the loudest frequency have also been used to recognize migratory birds (Schrama et al. 2007). Given that bird sound frequencies are distinctively high with most bird species having sound frequencies ranging from 1 to 8 kHz (Bonney 2007), sound frequency related predictor variables were commonly used for detecting bird sounds in recordings.

In this study, a logistic bird sound detection model using sound frequency percentiles was proposed as an alternative to CNN for automatic bird sound detection. The logistic model and sound frequency percentiles, descriptive parametric representations of sound frequency distribution of an audio recording, were chosen aiming to reduce the computational resources needed for training a detection model, and to use relatively interpretable predictor variables. Specific objectives were: 1) to test the effectiveness of using sound frequency percentiles in a logistic model to predict the presence of bird sounds in audio recordings, 2) to compare the performance of this approach to results from a CNN approach, and 3) to provide an open source algorithm to implement both detection models. This study provides an efficient and accurate algorithm for detecting birds from audio recordings that could potentially be used in a wide variety of environments.

2.2 Methods

2.2.1 Data

In 2016, the Institute of Electrical and Electronics Engineers (IEEE) Signal Processing Society initiated a Bird Audio Detection challenge (Stowell et al. 2016), offering a dataset in real live bioacoustics monitoring projects. The audio recordings dataset included 15,690 10-second recordings (Table 2-1). About half of the recordings were from a United Kingdom (UK) bird-sound crowd-sourced research spinout called Warblr (Warblr 2015). Warblr included smartphone-derived recordings covering a wide distribution of UK locations and environments. The other half of the recordings were from a world-wide field recording project called FreeSound (Stowell and Plumbley 2014). The recordings from FreeSound were diverse in location and environment from all around the world with a relatively high proportion taken in Europe. Each 10-second recording was categorized into bird presence or absence by a network of volunteers, including a revalidation process that minimized mislabeled recordings. Audio recordings covered a wide range of bird species (species information not provided in the dataset), and included noise due to weather, traffic, large mammals, insects, human speech, and even human bird imitations. All recordings were formatted into a 44 kHz sampling rate and the mono pulse code modulation WAV (Stowell et al. 2016).

Table 2-1 Number of audio recordings by data source and bird presence/absence.

	Presence of birds	Absence of birds	Total
Warblr	6,045 (39%)	1,955 (13%)	8,000 (52%)
FreeSound	1,935 (12%)	5,755 (37%)	7,690 (48%)
Total	7,980 (51%)	7,710 (49%)	15,690 (100%)

2.2.2 Audio processing and variable extraction

A high-pass filter with a cut-off sound frequency of 400 Hz was applied to each recording to reduce the low-frequency noise caused by wind or mechanical operation (de Oliveira et al. 2015). Each recording was then sliced into many short sound frames, with each sound frame being 12 milliseconds long with a 6 milliseconds overlap (i.e., the first frame contained 1–12 milliseconds, the second frame contained 7–18 milliseconds, etc.). The spectrogram (Figure 2-1a) was then generated by applying the discrete Fourier transformation to each sound frame (Boll 1979). The dominant sound frequency (i.e., the sound frequency with the highest intensity) was selected from each sound frame (Figure 2-1b) and these were used to obtain an empirical cumulative distribution (Figure 2-1c). Since bird sounds typically range from 1 to 8 kHz (Bonney 2007), it was hypothesized that the higher sound frequencies would be more powerful for detecting bird presence. Therefore, from the empirical cumulative distribution, 10 sound frequency percentiles (i.e., 30^{th}, 40^{th}, 50^{th}, 60^{th}, 70^{th}, 80^{th}, 90^{th}, 95^{th}, 97.5^{th}, and 99^{th}) were extracted as candidate predictor variables. More sound frequency percentiles were extracted in higher percentiles; furthermore, the source of the recording (i.e., Warblr or FreeSound), SOURCE, was added as an additional candidate predictor variable. This indicator variable was to account for the difference between the two sound projects (e.g., crowdsourcing, Warblr, using uncontrolled equipment versus remote monitoring project, FreeSound, using fixed and known recording equipment).

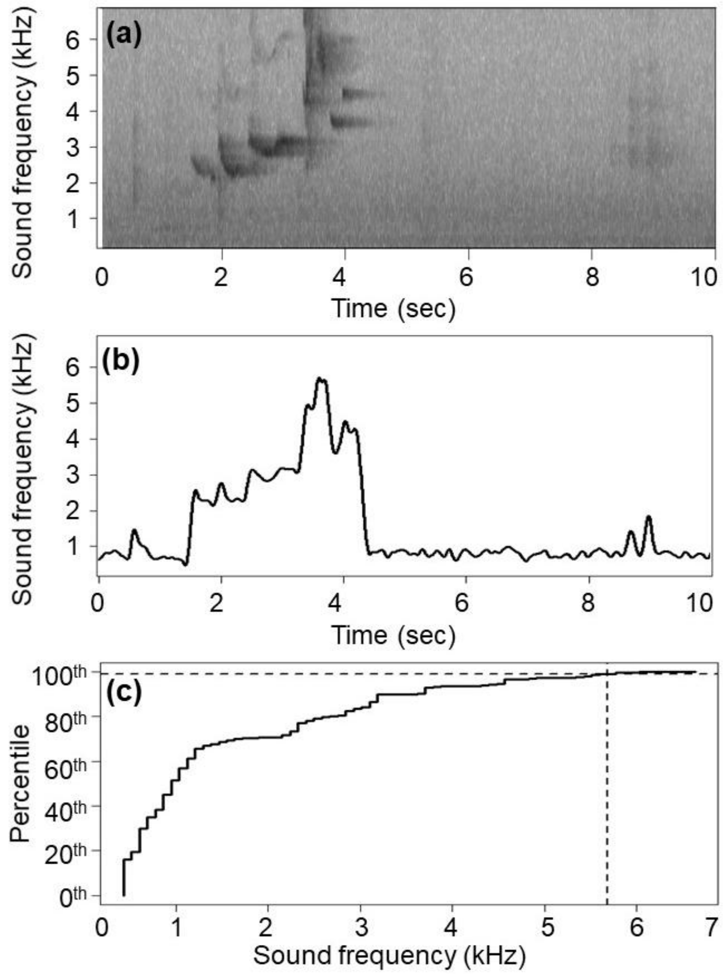

Figure 2-1 Process of extracting sound frequency percentiles from a recording. (a) Spectrogram of a ten-second long recording. (b) Dominant sound frequencies selected from each of the sound frames in the spectrogram. (c) Empirical cumulative distribution of dominant sound frequencies. The 99th percentile was marked by dashed lines for demonstration.

2.2.3 Logistic detection model formulation

Logistic models (McCullagh and Nelder 1989) were developed for bird detection from audio recordings, specifically:

$$Pr\hat{o}b(Y=1) = \frac{exp(\beta_0 + \beta_1 x_{1i} + \cdots + \beta_m x_{mi})}{1 + exp(\beta_0 + \beta_1 x_{1i} + \cdots + \beta_m x_{mi})}$$

where $Pr\hat{o}b(Y=1)$ is the predicted probability of a bird presence, $x_{1,\ldots,m}$ are predictor variables, and $\beta_{1,\ldots,}\beta_m$ are the parameters corresponding to each of the predictor variables. Model parameters were estimated using maximum likelihood (McCullagh and Nelder 1989) and the glm() function in R (R Core Team 2019), specifying a generalized linear model with a logit link and a binomial distribution.

A "base model" was first developed. Likelihood ratio tests (α=0.05) were used to test whether the candidate predictor variables (i.e., 10 frequency percentiles, SOURCE, and interactions between percentiles and SOURCE) contributed significantly to the detection of bird sound in audio recordings. Specifically, likelihood ratio tests were used to test: 1) whether to include any of the candidate variables, 2) whether to include SOURCE, and 3) whether to include interactions between percentiles and SOURCE. After selecting a base model using these tests, the possibility of further variable reductions was examined by applying backward stepwise selection (i.e., backwards elimination). Specifically, percentiles with their interactions with

SOURCE were dropped until all remaining percentiles with SOURCE interactions were significant (α=0.05).

2.2.4 Logistic detection model evaluation

Since the accuracy of a logistic model is often overestimated when using the same observations for model building and testing (Hosmer et al. 2013), the leave-one-out cross-validation method (Snee 1977) was applied. Specifically, the predicted probability for each recording was based on the model fitted without that particular observation. Accuracy metrics were selected based on recommendations for habitat models provided by Pearce and Ferrier (2000) and for acoustic recognizers provided by Knight et al. (2017).

First, the Hosmer-Lemeshow goodness-of-fit test (α=0.05) (Hosmer et al. 2013) was used to test the agreement between observed bird presence (i.e., true bird presence) and the predicted probabilities. The chi-square statistic was derived with a group number of 20, where the first group included audio recordings with 0 to 0.05 predicted probabilities. A significant p-value indicates model lack-of-fit.

The predicted presence or absence of each audio recording was obtained by comparing the predicted probability to a cut-off probability: an observation was categorized as predicted presence if the predicted probability ≥ cut-off probability. In order to assess how the cut-off probability influences the logistic detection model performance, overall accuracy, false negative rate, and false positive rate corresponding to each cut-off probability ranging from 0.2 to 0.9 in increments of 0.05 (Neter et al. 1996) were calculated.

$$Overall\ accuracy = Prob(Pred = 0|Obs = 0) + Prob(Pred = 1|Obs = 1)$$

$$False\ negative\ rate = Prob(Pred = 0|Obs = 1)$$

$$False\ positive\ rate = Prob(Pred = 1|Obs = 0)$$

where *Pred* and *Obs* were predicted and observed presences, respectively. A value of 1 indicates presence, and 0 indicates absence. The false negative rate indicated the chances of the model missing the bird sound in the recording, while the false positive rate indicated the chances of the model failing to filter the recordings without bird sound. An optimal cut-off probability was selected based on the highest overall accuracy.

Finally, the relative operating characteristic (ROC) curve was derived by plotting the true positive rate (i.e., 1-false negative rate) against the false positive rate across a gradient of cut-off probabilities (DeLong et al. 1988). Accordingly, the area under the ROC curve (AUC) was calculated as an aggregate measure of performance of a detection model: a model with an AUC above 0.7 and 0.8 provides satisfactory discrimination and excellent discrimination, respectively (Hosmer et al. 2013).

2.2.5 Comparison to a CNN detection model

A convolutional neural network (CNN) detection model was developed as a comparison to the logistic detection model. The CNN architecture was based on an eight-layer CNN from the Canadian Institute for Advanced Research (CIFAR-10) in Keras API (Chollet 2015). This CNN architecture was selected given its reported high accuracy in the CIFAR-10 classification task for image classification. The source code was provided by Lima (2018) and was further modified to process the audio recording dataset in this study. The input layer of the CNN included sound spectrograms derived from the 10-second recordings with each spectrogram downsized to a single channel image of a 50 Hz-by-50 second pixels to reduce the computer processing time. This CNN architecture included four convolution layers, two pooling layers, and two dense layers (Figure 2-2). For regularization, dropout (Srivastava et al. 2014) with a rate of 0.25 was employed in convolutional layers. The network was trained with 30 epochs (i.e., 30 full training cycles) and a batch size of 100 using the Adam optimizer (Kingma and Ba 2014) and binary cross-entropy as the loss function.

In order to compare the logistic model to the CNN detection model, the dataset was randomly partitioned into a training dataset (80%) and a test dataset (20%). Both the logistic and CNN models were fit using the training dataset and evaluated using the test dataset. The processing time to fit a model based on the training dataset and to make predictions on the test dataset was recorded for both types of models using a computer with an Intel Core i7-4790 CPU operating at 3.6 GHz. The overall accuracy, false negative, and false positive rates were calculated based on the predictions made using the models on the test dataset.

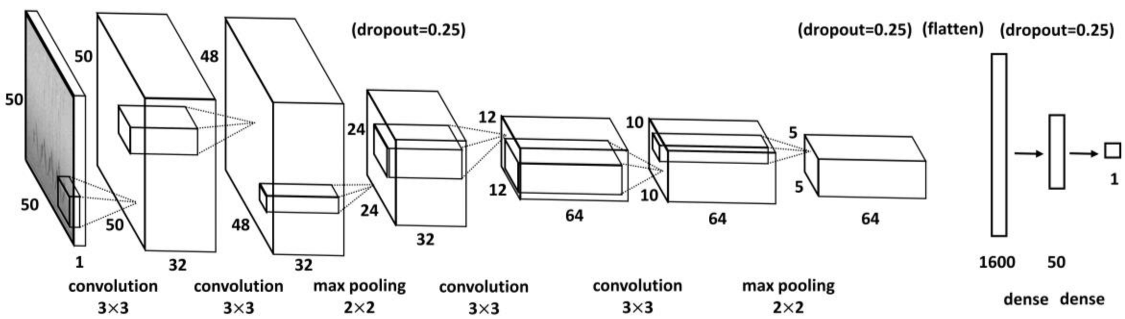

Figure 2-2 The complete convolutional neural network (CNN) model architecture used in this study. The numbers indicate the dimension of each object. The input layer of the model is the spectrogram of the recording and the output is the predicted probability of the presence of bird sounds.

2.3 Results

2.3.1 Characteristics of sound frequency percentiles

Two recordings were selected from the dataset to visually demonstrate the difference between audio recordings with and without bird sounds. The spectrogram of an audio recording with bird sounds had higher dominant sound frequencies compared to the one with human speech and traffic noise (Figure 2-3a). This difference in sound frequency distribution resulted in distinct patterns in the empirical cumulative distribution of the dominant sound frequencies (Figure 2-3b). The recording with bird sounds had a curve that rose steadily and achieved the 100th percentile with high sound frequency at around 6 kHz, while the recording without bird sounds had a curve that rose sharply and achieved the 100th percentile in low sound frequency at around 3 kHz.

Furthermore, 10 sound frequency percentiles were summarized using all recordings with and without bird sounds (Figure 2-4). The recordings without bird sounds had around 60% of dominant sound frequencies lower than 1 kHz and 90% of dominant sound frequencies lower than 2 kHz. In general, recordings with bird sounds had higher mean dominant sound frequency in each percentile than those without bird sounds.

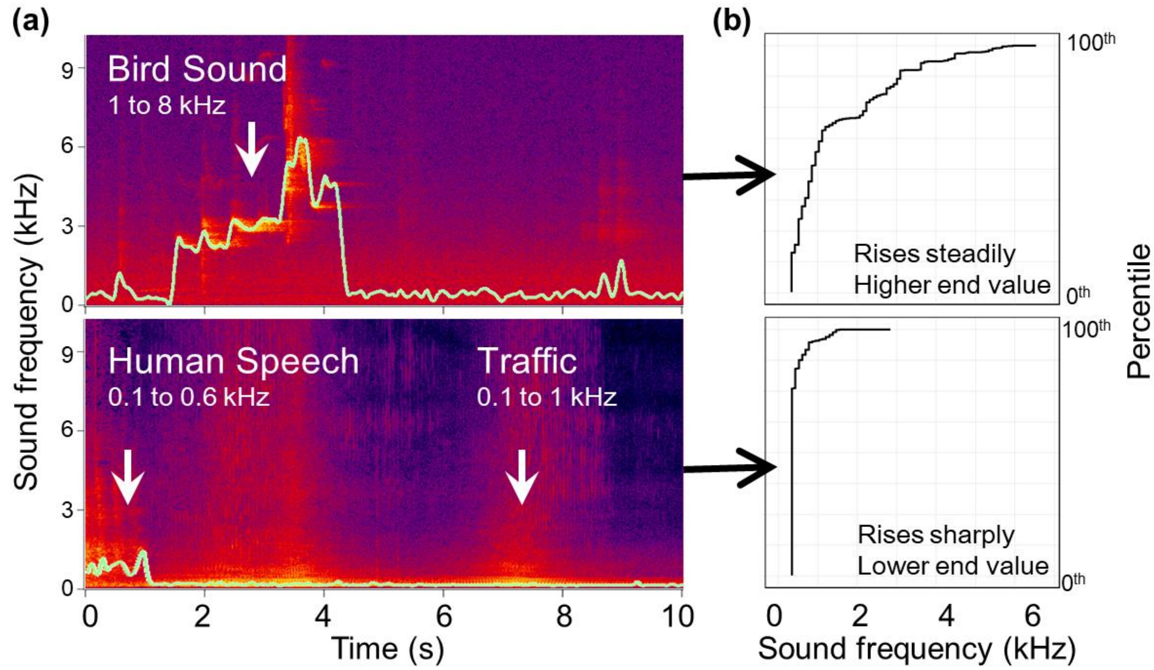

Figure 2-3 Illustration of audio recordings with and without bird sounds, specifically: (a) spectrograms of a recording with bird sounds (top), and a recording with human speech and traffic noise (bottom); and (b) associated empirical cumulative distributions of dominant sound frequencies.

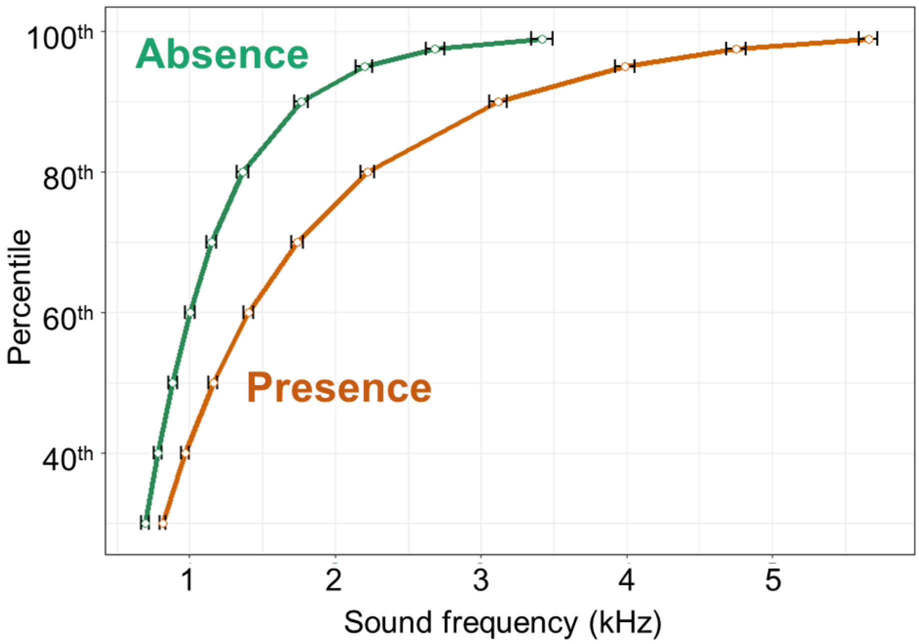

Figure 2-4 Sound frequency percentiles versus mean dominant sound frequencies with 99% confidence interval marked as horizontal error bars. Audio recordings were grouped by bird presence (orange) and absence (green).

2.3.2 Logistic detection models

To test the contribution of candidate predictor variables, four logistic models, the null model (GLM.0), two reduced models (GLM.R1, GLM.R2), and the full model (GLM.F), were fitted as possible base models (upper part of Table 2). All three models (GLM.R1, GLM.R2, and GLM.F) were significantly different from the GLM.0 based on likelihood ratio tests (α=0.05). Of these, GLM.F had the highest log likelihood and the lowest AIC. By comparing these three models using likelihood ratio tests, GLM.F was selected as the base model (i.e., a full model with all percentiles, SOURCE, and interactions between SOURCE and percentiles).

GLM.F was then reduced using backward stepwise selection (lower part of Table 2-2). The 40th, 80th, and 60th percentiles and their interaction with SOURCE were dropped sequentially (e.g., GLM.R3 was derived from GLM.F by dropping 40th percentile and its interaction with SOURCE). The final model, GLM.R5, included 15 predictor variables (i.e., 30th, 50th, 70th, 90th, 95th, 97.5th, and 99th percentiles, SOURCE, and the interactions of these percentiles with SOURCE).

Table 2-2 Logistic detection model comparison for selecting base model (upper part) and conducting variable selection based on the selected base model (lower part).

	Variables	Log likelihood	AIC	ΔAIC relative to GLM.0	p-value
GLM.0	None	-10873.2	21748	---	---
GLM.R1	10 percentiles	-9314.8	18652	3096	$< 2.2 * 10^{-6}$
GLM.R2	10 percentiles + SOURCE	-8105.8	16236	5512	$< 2.2 * 10^{-6}$
GLM.F	10 percentiles * SOURCE	-8043.9	16132	5616	$< 2.2 * 10^{-6}$
GLM.R3	9 percentiles * SOURCE (excluding 40^{th})	-8044.2	16128	5620	$< 2.2 * 10^{-6}$
GLM.R4	8 percentiles * SOURCE (excluding 40^{th} and 80^{th})	-8044.8	16126	5622	$< 2.2 * 10^{-6}$
GLM.R5	7 percentiles * SOURCE (excluding 40^{th}, 80^{th}, and 60^{th})	-8046.8	16126	5622	$< 2.2 * 10^{-6}$

2.3.3 Logistic detection model accuracy

The distribution of predicted probabilities using the leave-one-out cross-validation process was clearly left-skewed for recordings with bird sounds versus right-skewed for recordings without bird sounds (Figure 2-5). The recordings with bird sounds had a higher median predicted probability (0.72) compared to that without bird sounds (0.20). Furthermore, potential false predictions could be noticed on these distributions. Specifically, the small peak on the left side of the orange frequency distribution are recordings with bird sounds but having low predicted probability (i.e., potential false negative). Alternatively, the small peak on the right side of the green frequency distribution are recordings without bird sounds but having high predicted probability (i.e., potential false positive).

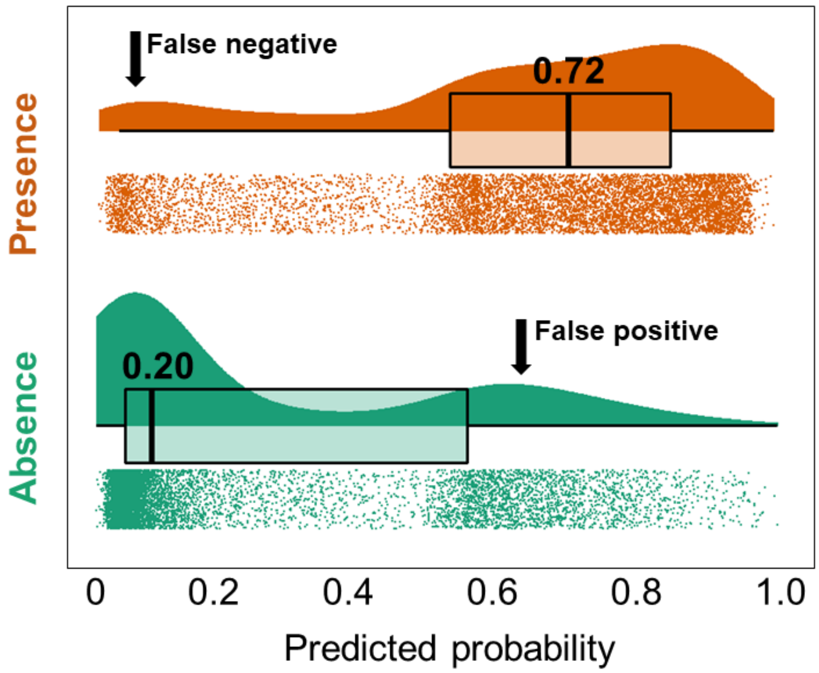

Figure 2-5 The distributions of predicted probabilities for recordings with (orange) versus without (green) bird sounds. The left and right side of the boxes are the first quantile (Q1) and the third quantile (Q3) of the predicted probabilities, respectively. The recordings with bird sounds had a higher median predicted probability (0.72) than that of recordings without bird sounds (0.20).

The Hosmer-Lemeshow test (α=0.05) were applied to test whether the predicted probabilities closely match the observed proportions of recordings with bird sound. The result indicated a lack-of-fit (p-value <0.001). However, it should be noted that the power of this test is very high given the large number of audio recordings; thus, even a small lack-of-fit would be detected. To illustrate this, the observed presence proportions were plotted against predicted probabilities for the 20 equal-interval probability groups (Figure 2-6). Generally, the observed presence proportions were higher than the predicted probabilities in the mid-range of predicted probabilities, indicating some lack-of-fit. This generally corresponded to the predicted probability groups with less data (i.e., shown as smaller blue bubbles). Further, the slope and the intercept of the fitted line were 0.96 (parameter standard error 0.05) and 0.03 (parameter standard error 0.03), respectively. The 1:1 correspondence fell in the region of the 95% confidence band, indicating the model was well-calibrated.

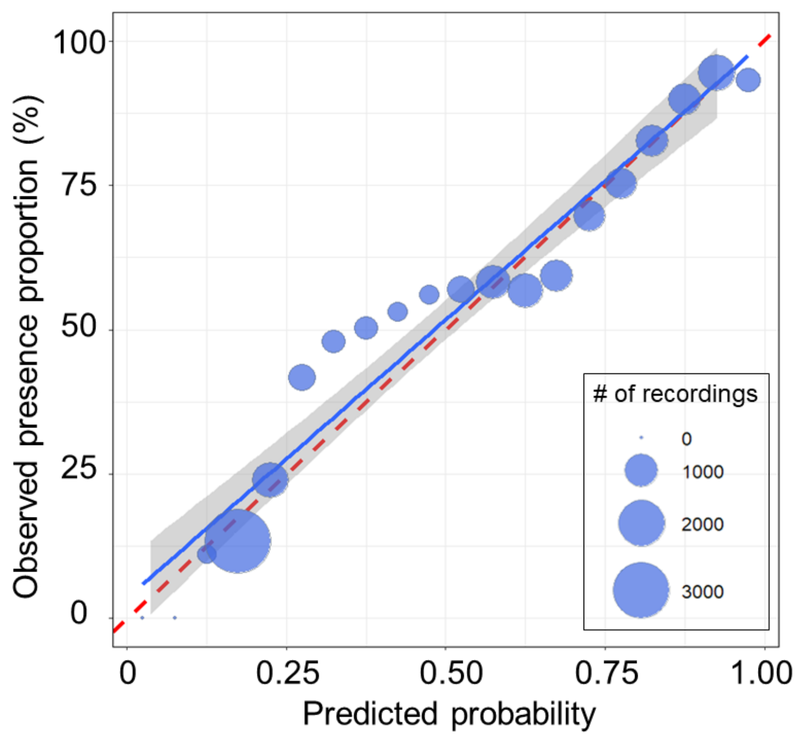

Figure 2-6 Observed presence proportions versus predicted probabilities for 20 equal-interval predicted probability groups (blue bubbles). The size of the bubbles represents the number of recordings in each group. The fitted line (solid blue line) is shown along with a 95% confidence band (gray area), compared with a 1:1 correspondence (dashed red line).

The overall accuracy, false negative, and false positive rates were calculated by varying cut-off probabilities from 0 to 1, by increments of 0.05, to show the effects of the varying cut-off probability (Figure 2-7). The optimal cut-off probability was 0.35 based on the highest overall accuracy of 75% (31% true positives and 44% true negatives). The corresponding false negative rate was 16%, with a false positive rate of 35%. Finally, the model achieved an AUC of 82%, showing that the model provided excellent discrimination between recordings with and without bird sounds.

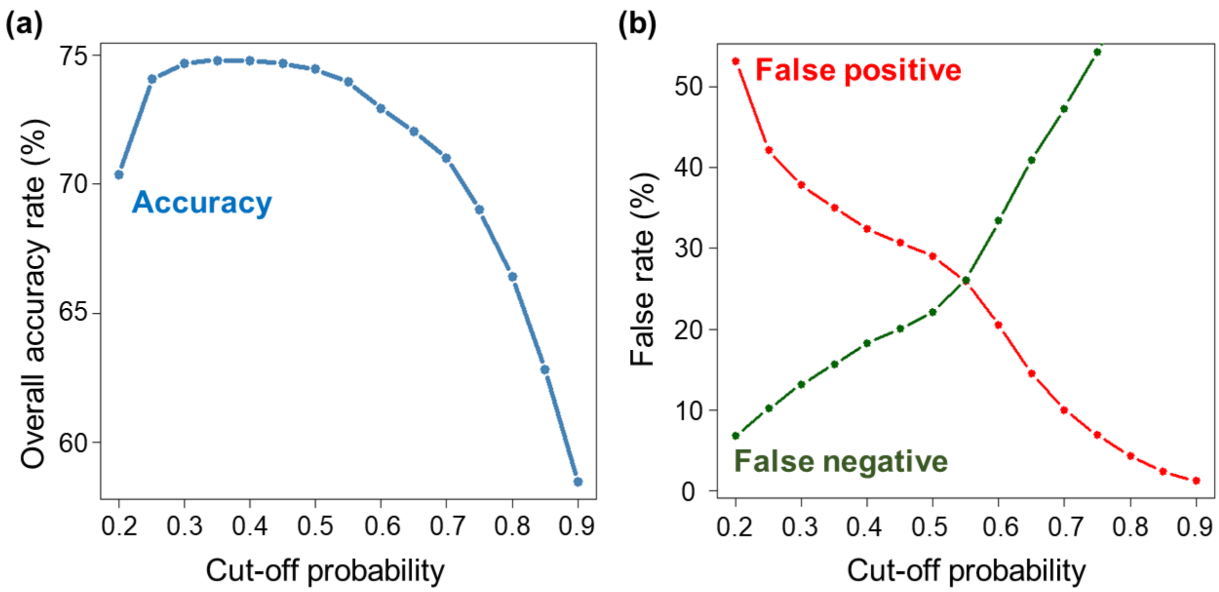

Figure 2-7 (a) Overall accuracy (blue), (b) false negative rate (green), and false positive rate (red) across a gradient of cut-off probabilities.

2.3.4 Logistic versus CNN models

The logistic and CNN models were compared by partitioning the dataset into a training dataset (80%) and a test dataset (20%). The processing time for the logistic model was shorter than that of the CNN model for both training and making predictions (Table 2-3). In particular, each 10-second recording required around 0.3 seconds to make predictions using the logistic model versus 2 seconds using the CNN model. However, the logistic model had a slightly lower overall accuracy than CNN model with a higher false positive rate, and a similar false negative rate.

Table 2-3 Processing times and model performance comparison between the logistic model and the CNN. Processing times were tested on a computer with an Intel Core i7-4790 CPU operating at 3.6 GHz.

Model	Processing time for training (hr)	Processing time for making predictions (hr)	Overall accuracy	False negative	False positive
Logistic	1:09	0:17	76%	14%	34%
CNN	6:48	1:40	84%	19%	13%

2.4 Discussion

2.4.1 Using sound frequency percentiles as low-level descriptive parametric representations

It was hypothesized that high sound frequency percentiles would be powerful for detecting bird presence in audio recordings based on the fact that bird sound has distinctively high sound frequencies (Bonney 2007). This hypothesis was supported by our result, where a logistic detection model with high sound frequency percentiles achieved an overall accuracy of 75% in detecting bird sounds in audio recordings. The predictive power of each percentile was determined by the significance level of the coefficients (Hosmer et al. 2013), which enables variable selection and interpretation of the model.

2.4.2 Challenges of CNN detection models

Despite achieving high overall accuracy, CNN models have several potential disadvantages when used to detect bird sound. First, the simplification of spectrograms as images might result in the loss of information. The input of the CNN model were the spectrograms of the audio recordings, which have very different meanings in the axes: sound frequency (Hz) versus time (second). Although treating spectrograms as images (i.e., with same meaning of axes) in CNN models has become a common approach for sound detection tasks and proved to be extremely useful (Stowell et al. 2016), some information, such as harmonics of sounds, might be missed with the strong localization ability of CNN models. Second, interpretability of the CNN model was limited. Although the large number of parameters in a CNN enable it to model nonlinear relationships in the data, they also limit the interpretability of the CNN model since the contribution of the kernels in each convolution layer is difficult to determine (Dreiseitl and Ohno-Machado 2002). Finally, the CNN model required seven times more computational resources than the logistic mode, even with a relatively simple CNN architecture. A "deeper" CNN model (i.e., a CNN model with more convolution layers) might provide even better model performance, but would require greater processing resources. This would be especially of a concern where the processing resources are limited. In this case, the logistic detection model is relatively simple, easier to modify, and can be applied readily to large datasets.

2.4.3 Challenges of logistic detection models

Although having several advantages over the CNN model, the logistic detection model still had some potential limitations. First, the detection model might not be useful for audio recordings collected during high sound activities, such as dawn recordings in bird abundant areas (e.g., boreal forests), where majority of recording periods are with bird sounds and a pre-filtering step is not necessary. Second, the logistic detection model might miss the bird species with extreme low sound frequency (e.g., owl, grouse, ptarmigan), given that more high sound frequency percentiles were selected in the model. Further, the logistic detection model also got high false positive (35%) and false negative (16%) rates. For these false predictions, false positives would increase the examination effort after applying the detection model, but would not influence the truthfulness of the following analysis as the recordings of interest would be retained in the sample. In contrast, false negatives were likely to become an issue. The recordings were predicted to have bird absence, whereas they might include important information, particularly in the case that ‘filtered out’ recordings of a species of interest. This approach might still work if these ‘filtered out’ recordings do not include the target group of species being monitored.

False positives likely resulted from the inclusion of non-bird but high frequency sounds occurring in this diverse dataset, such as insect vocalizations. For example, cicadas have their sound frequency ranges from 4 kHz to 16 kHz (Bennet-Clark and Young 1994) overlapping with the range for birds of 1 to 8 kHz (Bonney 2007). As a result, using upper frequency percentiles in the logistic model may not have recognized the cicadas as non-bird sounds. This issue with cicada sounds affecting the performance of a bird sound detection model has been noted in other research (Towsey et al. 2014). A solution for this issue was proposed by Brown et al. (2019), where nine acoustic indices were used to filter cicada chorus in a recording. Towsey et al. (2014) also used spectral entropy and background noise to develop a simple classifier to detect cicadas. Instead of manually checking and identifying the false positives from the logistic model results, these insect sound detection algorithms could be applied after the bird sound detection model to reduce the false positives and save time examining all recordings predicted as including bird sounds.

False negatives likely resulted from the inclusion of unconstrained content (e.g., wind, rain, traffic noise) which masks bird sounds (Rumsey and Mccormick 2012). In the logistic detection model, the dimension reduction approach for calculating predictor variables involved the selection of the dominant sound frequency in a specific sound frame. This approach has limited ability in detection if there were other sound sources having higher intensity than that of bird sounds at the same sound frame. For this, one solution is to integrate other predictor variables into the logistic detection model that are more robust when multiple sound sources exist in the same sound frame. Another solution is to filter the unconstrained content in the recording before applying the detection model. In particular, several indices have been proposed for this filtering purpose, such as the acoustic complexity index (Pieretti et al. 2011), spectral and temporal entropy (Sueur et al. 2008), background noise (Towsey 2013), and spectral cover (Towsey et al. 2014).

2.4.4 Data science for making predictions

Both statistical and machine learning models can be used to build predictive models, as demonstrated in this study. The selection of a model form for building predictive models depends not only on high overall accuracies, but also on the ability of the model in preventing overfitting, or overtraining in machine learning (Srivastava et al. 2014). Overfitting indicates that model predictions are too exact to a particular set of data, and may fail to accurately predict future observations (Schaffer 1993), which might result from the inclusion of irrelevant variables or to use a model form that is more flexible than it needs to be (Hawkins 2003). A machine learning model is more vulnerable to overfitting given numerous parameters in a model (typically more than thousands), which, on the other hand, enable a machine learning model to discover complicated nonlinear relationships underlying the data (Srivastava et al. 2014).

Several techniques were used in this study to prevent potential overfitting issues. For the logistic models, overfitting was prevented by examining the correlation between predictor variables and with a careful variable selection process, such as the controlled stepwise selection (i.e., backwards elimination) (Ramsey and Schafer 2013). For the CNN models, overfitting was prevented by drop out (Srivastava et al. 2014) and by splitting part of the training dataset into validation dataset for tuning parameters in the training stage (Geron 2017). Overall, both statistical and machine learning models have corresponding strategies to prevent overfitting, making both model forms suitable for developing predictive models. Thus, future challenges for predictive models will be how to keep the high accuracy that machine learning models achieved, while also increasing the interpretability and reducing required computational resources.

2.4.5 Future work

Covering a wide range of bird species and ecosystems, the audio recordings used in this study provided an opportunity to build a model with broad potential applications. However, the lack of information about bird species in the dataset limited the possibility of examining the model performance across different bird species groups. Thus, future studies are needed to test this logistic detection model on audio recordings focusing on finding different target species. For this, a better model performance is expected given decreased variation in the data.

2.5 Conclusions

A logistic detection model with frequency percentiles was developed aiming to use relatively simple and interpretable predictor variables, to reduce the computational time needed, and to simplify the process of making/revising new acoustic detection models. Using sound frequency percentiles in a logistic model can accurately predict the presence of bird sounds in audio recordings (i.e., 75% overall accuracy rate and 82% AUC), even given a large variability in the datasets. Further, the processing speed was over seven times faster than using the CNN model, indicating the potential of this approach as a pre-filtering step within an overall bird identification algorithm. In particular, a pre-filtering step has potential to greatly reduce the time required to process audio recordings by eliminating the periods of recordings without bird sounds.

The R code for the logistic model, the CNN model, and example recordings are available on GitHub (https://github.com/SunnyTseng/Bird-Sound-Detection-2019.git, accessed on September 20, 2019).

Chapter 3: Previous fire severity enhances reburn severity: a case study in interior British Columbia, Canada

3.1 Introduction

Forest wildfire is a common natural disturbance in British Columbia (BC), Canada (Daniels and Gray 2006). Forests in interior BC, specifically forests in the Interior Douglas-fir Biogeoclimatic Zone (IDF) (Meidinger and Pojar 1991), are naturally maintained by wildfires, leading to open uneven-aged stands interspersed with gaps of grass and shrub lands (Province of BC 1995). Over the past several centuries, the IDF experienced mixed severity fire regimes that resulted from the influence of climate, fuels, topography (Marcoux et al. 2015), with surface fire frequency ranging from 4 to 50 years and crown fires occurring at 150 to 250 year intervals (Heyerdahl et al. 2012, Province of BC 1995). Combined effects of human land use, fire suppression, and climate variation then influenced this fire regime (Daniels et al., 2013). Wildfire characteristics have been shifting with climate change, where longer, warmer, and drier summers may alter the existing fire regimes (Daniels et al. 2017).

BC has recently experienced unprecedented fire seasons in terms of the total number of fires, total cost of fire suppression, and total areas burned (BC Wildfire Service 2019). In the summer of 2017, more than 1.2 million hectares of area were burned in BC, influencing human health, ecosystem services, environment, and biodiversity (BC Wildfire Service 2017). Fire seasons have started earlier and lasted longer, representing the "new normal" in BC, as a part of the global trend of increasing fire activities (Daniels et al. 2017). For this, resources have been devoted to developing and applying innovative post-fire management strategies, in order to lower the probability of subsequent fire events and lower the severity of subsequent fires when they occur (Daniels et al. 2017).

Previous fires affect rates of fuel consumption and accumulation, thus influencing the probability and severity of subsequent fires (hereafter: reburn) (Harvey et al. 2016). The ability of past states of an ecosystem to influence future ecological responses has been termed ‘ecological memory’ (Sun and Ren 2011). Studies about ecological memory in successive fires have revealed varied relationships: previous fires may limit (Teske et al. 2012, Parks et al. 2015) or enhance (Collins et al. 2009, Thompson et al. 2007, van Wagtendonk et al. 2012) the reburn severity, thus yielding findings that may be valid only for a particular ecoregion. There is limited information regarding how the severity of previous fire influences the reburn severity in interior BC; however, this information is becoming more important as changes in climate are likely to alter current fire regimes in the area and lead to shorter fire return intervals (Daniels et al. 2017). Identifying factors that drive reburn severity could potentially help in advising management activities to mitigate damage from subsequent fire events (Dunn and Bailey 2015).

Several permanent plots in the Riske Creek area in interior BC were burned twice: first in 2009 or 2010 and a second time by the 2017 Hanceville fire (BC Wildfire Service 2019). Plots were located in two different forest patch types: 1) fragmented forest patches, where small patches of trees were interspersed with grasslands, and 2) continuous forest patches, formed by a single large stand of trees. Fire behaviour and fire characteristics may differ among forest patch types due to differences in stand structure, such as species composition, tree density, and tree size (Fernandes 2009). Previous field data, including tree species, size, and condition (live or dead), were available for pre- and post-first fire (i.e., 2009 and 2010 fires), which enabled quantifying the first fire severity. To assess reburn severity, additional soil data were collected in 2018, one year after the 2017 reburn.

In this study, an ordinal model was used to determine whether and how the severity of previous fire influenced the reburn severity in the Riske Creek area in interior BC. Specific objectives were: 1) to describe and compare the pre-first fire stand structure, including species composition, tree density, and basal area, between continuous and fragmented forest patches, and 2) to identify whether the severity of the first fire, which was represented by basal area and density metrics, enhances or limits the reburn severity. By identifying the relationship between severities, the results of the study may be used to inform post-fire management strategies that are implemented to lower the probability of reburn and lower the reburn severity if a reburn occurs.

3.2 Methods

3.2.1 Study area

The study area is near Riske Creek (51°52’ N, 122°21’ W), in the Very Dry Warm Interior Douglas-fir (IDF) Biogeoclimatic Zone (Meidinger and Pojar 1991), approximately 50 km west of Williams Lake, British Columbia, Canada. Elevation of the study area ranges from 920 to 990 m with a mixture of deciduous and coniferous species embedded in a matrix of grasslands, shallow ponds, and wetlands. Trembling aspen (*Populus tremuloides* Michx.) is the major deciduous species, and predominant coniferous species are lodgepole pine (*Pinus contorta* Douglas ex Loudon var. *latifolia* Engelm. ex S. Watson), Douglas-fir (*Pseudotsuga menziesii* (Mirb.) Franco var. *menziesii*), and white spruce (*Picea glauca* (Moench) Voss). Forest habitat details are given in Martin et al. (2004). Five sites were included in the study: Military Gate (MG), Rock Complex (RC), Rock Lake (RL), Rock Pine (RP), and Solitary Woods (SW) (Figure 3-1, Table 3-1).

An outbreak of mountain pine beetle (*Dendroctonus ponderosae*) began in the study area around 1998, peaked in 2003 and 2004, and killed most lodgepole pine trees (Drever et al. 2009). Salvage logging in 2007 and 2008 further affected the stand structure by removing the majority of dead pine trees (Edworthy and Martin 2013). Meanwhile, in 2008, trees over one meter tall and under 20.3 cm in diameter were knocked down at site RP for grassland restoration by the Range Branch of the BC Ministry of Forests, Lands and Natural Resource Operations (Cariboo-Chilcotin Grasslands Strategy Working Group 2007). Then, three large wildfires occurred in the study area and, as a result, most of the area was burned twice: two fires in 2009 and 2010 (hereafter: first fire) occurred in the southern and northern parts of the study area, respectively. Post-fire logging was conducted in site MG, specifically in nine plots dominated by Douglas-fir, where all trees regardless of size and species were cut. After the logging, Tolko Industries Ltd.

replanted these plots with lodgepole pine seedlings in a density of 1,400 seedlings per hectare (G. Glessing, personal communication, October 11 2019). The areas burned by the first fire were then burned again by the 2017 Hanceville fire (hereafter: reburn) (BC Wildfire Service 2019) (Figure 3-1, Table 3-1). Site summary statistics including species composition are provided for different years to illustrate the stand structural change due to fires: upon the establishment of sites in 1990s (Table A-1), post-first fire (Table A-2), and post-second fire (Table A-3).

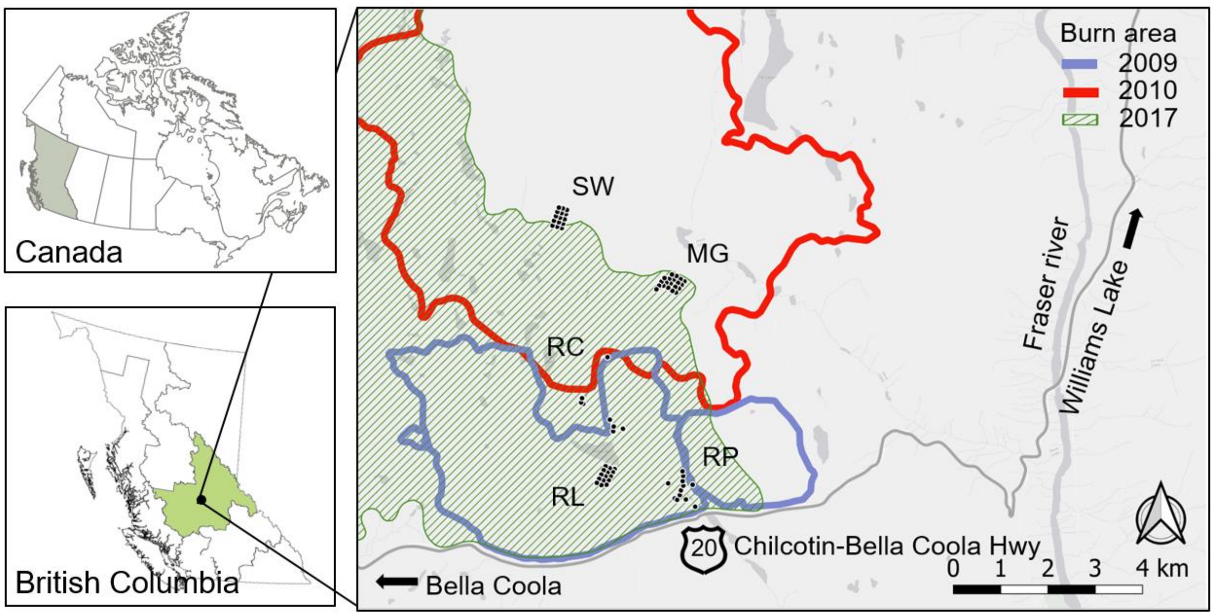

Figure 3-1 Burn area of the three wildfires and location of the five study sites: Military Gate (MG), Rock Complex (RC), Rock Lake (RL), Rock Pine (RP), and Solitary Woods (SW). Each of the five sites was composed of a cluster of plots (black dots).

Table 3-1 Tree basal area per hectare (BA), percent BA by species, and mean, standard deviation (SD), and maximum (max) diameter at breast height (DBH) prior to the first fire: 2008 measurement for RC, RL, RP and 2010 for MG, SW. Species code: trembling aspen (AT), lodgepole pine (PL), Douglas-fir (FD), spruce sp. (Sx). Numbers in bold font indicate the dominant tree species on each site.

Site	Year of 1st fire	Year of reburn	BA	AT % BA	PL % BA	FD % BA	Sx % BA	mean DBH	SD DBH	max DBH
MG	2010	2017	574	17	7	**75**	1	20.9	10.9	92.0
RC	2009	2017	118	29	**62**	9	0	22.3	8.80	51.5
RL	2009	2017	222	4	29	**60**	7	22.8	8.47	57.5
RP	2009	2017	207	10	**67**	23	0	20.7	11.0	105.0
SW	2010	2017	234	11	11	**78**	0	21.1	9.77	68.4

†sites in continuous forest patches have plots established from the edge and extended into the forest. Sites in fragmented forest patches have plots established in a series of “forest islands

3.2.2 Data collection

A total of 70 plots within five sites were established between 1995 and 1997. Each site included 10 to 15 circular plots (radius 11.28 m) located in either continuous or fragmented forest patches (Table 3-2). The sites in continuous forest patches had 11.28 m radius plots established systemically on transects from the edge into the interior of the forest, with plot centres 100 m apart. The sites in fragmented forest patches had plots established in a series of "forest islands" with each plot at least 50 m away from the forest edges and at least 100 m apart from each other. Details for the plot design are provided by Martin and Eadie (1999).

Plots were measured every year since their establishment in the 1995 (site RP in 1997) until 2011. All vegetation surveys were conducted during the growing season from May to August. Tree species, status (i.e., live or dead), and diameter at breast height (i.e., 1.3 m; DBH) for all trees greater than 12.5 cm in DBH were recorded. Plots were re-measured in the summer of 2018. For this latest measurement, surface organic matter (i.e., duff and litter) percent cover on the entire plot was assessed by ocular estimate (Forest Inventory and Analysis 2017). Surface organic matter included any needles, twigs, branches, seed cones, and a soil layer dominated by organic material (Forest Inventory and Analysis 2017).

Table 3-2 Forest patch type of each site, number of total plots, plots that were experienced by mountain pine beetle (MPB), and plots that were salvaged due to the mountain pine beetle outbreak or the grassland restoration (managed pre-1st fire).

Site	Forest patch type	# of plots	# of MPB plots	# of managed plots pre-1st fire
MG	Continuous	20	18	1
RC	Fragmented	8	8	1
RL	Continuous	15	11	8
RP	Fragmented	12	10	2
SW	Continuous	15	7	0

3.2.3 Response and explanatory variables

Response variable—Reburn severity was determined based on the soil fire severity as described by Jain et al. (2012), with the abundance of post-fire surface organic matter as the criterion to classify fire severities. Based on this, each plot was categorized into one of four soil fire severities (Figure 3-2, Table 3-3).

Mountain pine beetle, salvage logging/grassland restoration, and forest patch type—Three binary explanatory variables were included as candidate explanatory variables to account for the effects of mountain pine beetle, salvage logging, and forest patch type. A plot was categorized as attacked by mountain pine beetle if pine mortality was 100% during 1998 to 2008. Furthermore, a plot was defined as salvage-logged or experienced grassland restoration if any of the standing pines had been cut between 1998 and 2008. Finally, a forest patch type explanatory variable was included to indicate whether the plots were located in continuous or fragmented forest patches.

Stand structure—Thirty-six candidate explanatory variables were calculated to account for the pre-/post-first fire stand structure and the stand structural change caused by the first fire. Twelve metrics were used: total trees per hectare (TPH) and basal area per hectare (BA) were calculated by tree status (live versus dead). For living trees, BA and TPH were further calculated by tree species (conifer versus aspen), and tree size (large versus small) with a DBH threshold of 20 cm, the median DBH of all trees in the study area. These twelve metrics were calculated for the measurements before the first fire (2008 for RC, RL, RP and 2010 for MG, SW) and after the first fire (2010 for RC, RL, RP and 2011 for MG, SW). Additionally, the relative change of each metric was also calculated based on values before and after the first fire:

$$relative\ change = \frac{S_{post} - S_{pre}}{S_{pre}}$$

where, S_{pre} and S_{post} are the stand structure metrics before and after the first fire, respectively. Instead of using soil fire severity, as was done for the reburn, here the relative change stand structure explanatory variables were obtained as a proxy of the severity of the first fire (Collins et al. 2018). This was due to the lack of surface organic matter information after the first fire.

Table 3-3 Soil fire severity classification key for the reburn severity.

Soil characteristics	Soil fire severity
No evidence of a recent fire	0
Surface organic cover ≥ 85 %	1
Surface organic cover ≥ 40 % and < 85 %	2
Surface organic cover < 40 %	3

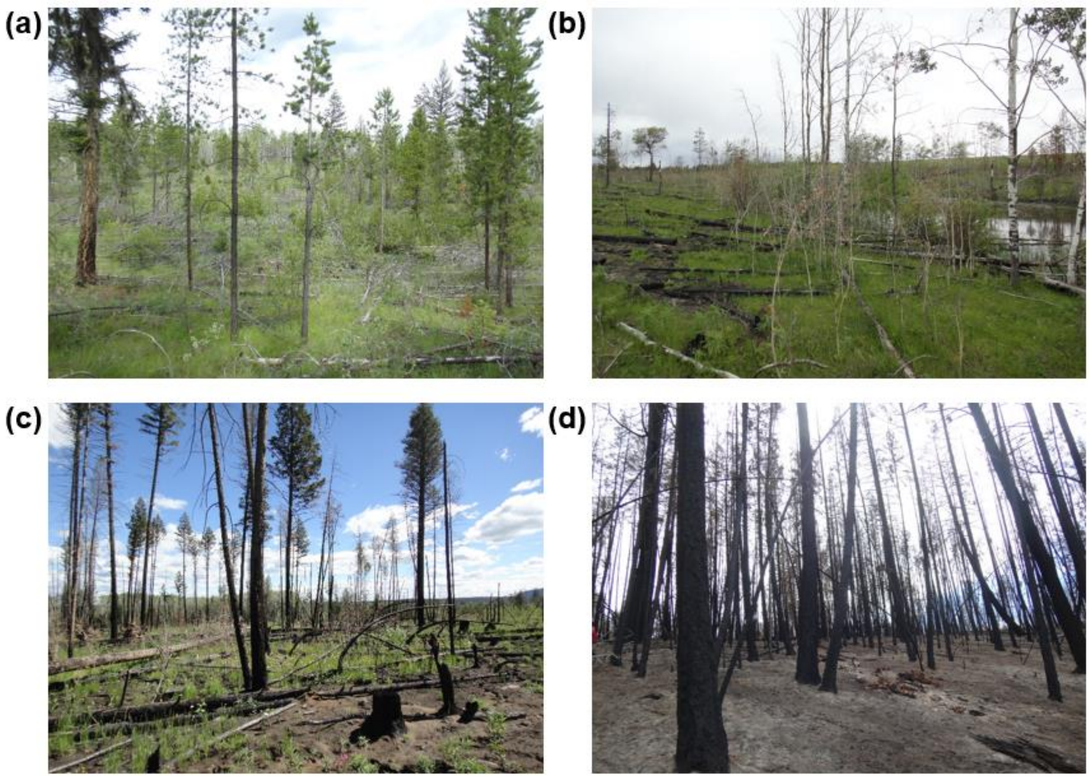

Figure 3-2 Examples of soil fire severity categories a) no evidence of a recent fire, b) surface organic cover ≥ 85 %, c) surface organic cover ≥ 40 % and < 85 %, and d) surface organic cover < 40 %, respectively (Refer to Table 3-3 for details).

3.2.4 Pre-first fire stand structure in two forest patch types

The pre-first fire stand structure explanatory variables were used to investigate the difference and the variability between pre-first fire conditions in the two forest patch types (i.e., continuous versus fragmented). The mean and the variance of the pre-first fire stand structure explanatory variables were calculated by forest patch type. Then, the difference between means and variances for each of the stand structure explanatory variables were tested using two-sampled t-tests (Student 1908) and Levene's test (Levene 1960), respectively.

3.2.5 Ordinal logistic model

The reburn severity, ranging from 0 to 3, can be considered as ordinal data. Therefore, an ordinal logistic model (McCullagh 1980) with cumulative odds was applied to relate the reburn severity to the explanatory variables that represent the mountain pine beetle outbreak, the salvage logging, pre-/post-first fire stand structure, and the stand structural change caused by the first fire. The cumulative odds compare the probability of an equal or smaller response with the probability of a larger response, both conditional on the explanatory variables:

$$\frac{P(Y \leq k|\boldsymbol{x})}{P(Y > k|\boldsymbol{x})} = exp(\alpha_k - \boldsymbol{x}'\boldsymbol{\beta})$$

where $P(Y \leq k|\boldsymbol{x})$ is the probability of a reburn severity being equal or smaller than level k, $\boldsymbol{x}'$ is a matrix of explanatory variables, α_k and $\boldsymbol{\beta}$ are model coefficients, and *exp* is the inverse of the natural logarithm. Note that the intercept coefficients were different across reburn severity levels while the slope coefficients were the same based on the proportional odds assumption (i.e., parallel regression assumption) (Wolfe and Gould 1998). Model parameters were estimated using maximum likelihood (McCullagh and Nelder 1989) with clmm() in R package “ordinal” (Christensen 2019).

First, a null model with no explanatory variables was fit to provide a baseline model. Then, univariable models were fit to examine the importance of each candidate explanatory variable (Hosmer et al. 2013). A random site effect was included to account for the variation among sites. Forward selection was applied based on Cox and Snell R^2 (Cox and Snell 1968), Akaike Information Criterion (AIC), and log likelihoods (Tabachnick and Fidell 2019). Variables were added until at least one variable in the model was not significant (α=0.05). Finally, interactions among variables were tested using likelihood ratio tests (α=0.05). The final model was evaluated with the overall accuracy and the Kappa statistics, which measure the agreement between observed and predicted reburn severities (Cohen 1960).

3.3 Results

3.3.1 Stand structure and species composition before the first fire

Initial measurement of the study area in the 1990s indicated that the dominant species, based on basal area per hectare (BA) across sites was Douglas-fir (~181 trees per hectare (TPH), 52% of BA), followed by lodgepole pine (~168 TPH, 35% of BA) and trembling aspen (~66 TPH, 12% of BA). The mountain pine beetle outbreak started in 1998 and killed most of the pine trees in 2003 and 2004, thus decreasing the number of live pines (green line in Figure 3-3 (a) and (b)). Furthermore, grassland restoration occurred in 2008, and salvage logging occurred during 2007 and 2008 (Figure A-1), thus decreasing the number of dead pines (green line in Figure 3-3 (b)). The density in both live and dead trees did not change greatly in Douglas-fir and trembling aspen (Figure 3-3).

Difference and variability between two forest patch types were examined using pre-first fire stand structure variables. With the exception of dead tree TPH and BA, all variables had a higher mean and variance in continuous than in fragmented forest patches (Table 3-4). Further, all variables were significantly different in means and variance, with exceptions for aspen and dead tree variables. The mean value of aspen and dead tree variables were not significantly different (α=0.05), given the high standard deviation (i.e., high variation across plots within site).

Table 3-4 t-test for comparing the mean, and Levene's test for comparing the variance of pre-first fire stand structure in two forest patch types. The p-values in bold font indicate the pairs with significant differences (α=0.05).

Variable	p-values of t-test	p-value of Levene's test	Mean (SD) in continuous forest patch (3 sites 50 plots)	Mean (SD) in fragmented forest patch (2 sites 20 plots)
Live tree TPH†	**<0.0001**	**0.0001**	332 (278)	109 (134)
Dead tree TPH	**0.0088**	0.2101	136 (123)	260 (180)
Live small tree TPH	**0.0045**	**0.0139**	184 (193)	75 (110)
Live large tree TPH	**<0.0001**	**0.0006**	148 (148)	34 (44)
Live aspen TPH	0.7517	0.7426	87 (185)	75 (122)
Live conifer TPH	**<0.0001**	**0.0009**	244 (272)	34 (81)
Live tree BA‡	**0.0025**	**0.0117**	14.1 (12.4)	5.16 (9.79)
Dead tree BA	0.0557	0.5661	6.46 (7.79)	11.1 (9.07)
Live small tree BA	**0.0008**	**0.0039**	3.36 (3.44)	1.18 (1.73)
Live large tree BA	**0.0116**	**0.0301**	10.8 (11.09)	3.98 (9.13)
Live aspen BA	0.9933	0.9526	2.22 (4.02)	2.22 (3.13)
Live conifer BA	**0.0029**	**0.0059**	11.9 (12.8)	2.94 (9.88)

†trees per hectare; ‡basal area

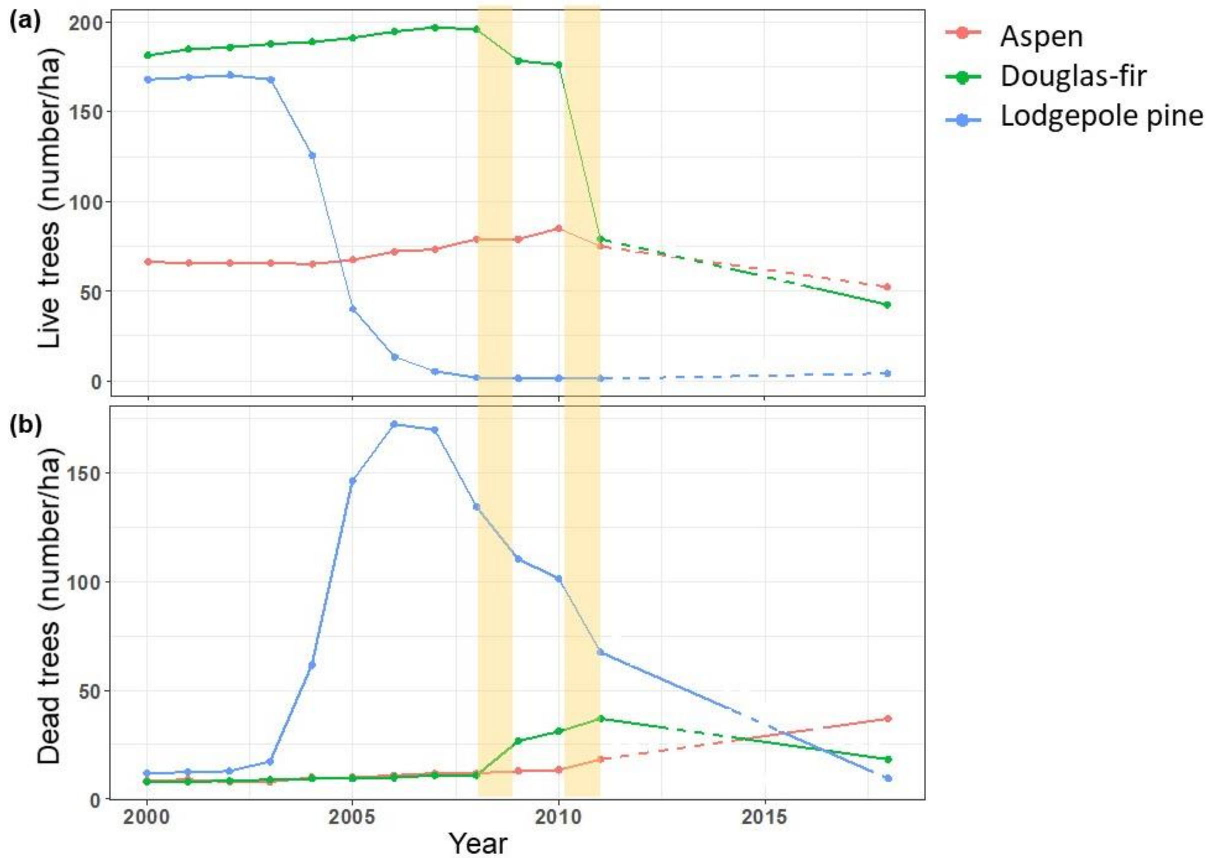

Figure 3-3 (a) Live and (b) standing dead tree density (trees per hectare, TPH) of the three dominant tree species in the study area. TPH was influenced by mountain pine beetle outbreak, post mountain pine beetle salvage logging, grassland restoration, and fires in 2009/2010 (highlighted in yellow). No measurements were available between 2012 and 2017. Therefore, the period is represented with dashed lines.

3.3.2 Reburn severity and the explanatory variables

Categories 0, 1, and 2 were distributed across sites. A total of 19 (27%), 29 (41%), 16 (23%), and 6 (9%) plots had reburn severity categories 0, 1, 2, and 3, respectively. Plots experienced post-first logging and replanting in site MG were mostly severely burned (Figure 3-4). A total of 54 plots were attacked by mountain pine beetle; after that, 12 plots out of the 54 experienced salvage logging or grassland restoration (Table 3-2). Correlations among the 36 stand structure explanatory variables were examined. Some variables were highly correlated with each other, such as relative change of live tree TPH and relative change of live small tree TPH (correlation coefficient=0.95), and relative change of live tree TPH and relative change of live conifer TPH (correlation coefficient =0.88). Thus, to avoid any multicollinearity issues, forward selection was applied in building the ordinal logistic model.

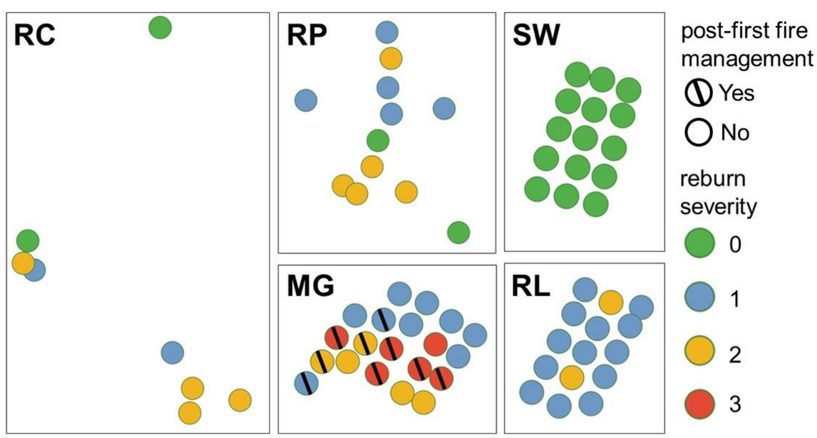

Figure 3-4 Spatial distribution of post-fire management and the reburn severity categories in each of the five sites. Refer to Table 3-3 for the soil fire severity classification key.

3.3.3 Reburn severity modelled by stand structural variables

After a process of variable selection, the reburn severity was modelled as a function of relative change of live tree BA, relative change of live small tree TPH, their interaction, and post-first fire live conifer BA (Table 3-5). This final model was superior to the null model (α=0.05), with a Cox and Snell R^2 of 0.29 and an AIC of 128.4. Higher decrease of live tree BA due to the first fire was associated with higher reburn severity. Specifically, one unit decrease in relative live tree BA was associated with a multiplicative increase of 42.9 (exponential of 3.759) in the odds of a plot falling above a certain fire severity level, when all other variables in the model being held constant (Table 3-5). Further, relative change of live small tree TPH, its interaction with relative change of live tree BA, and post-first fire live conifer BA had positive estimated coefficients, meaning higher variable values were associated with higher reburn severity. Note that relative change of live small tree TPH was included given its significant interaction with relative live tree BA.

Probabilities of the four reburn severity categories were predicted for each plot using the final model and the predicted reburn severity was defined as the category with the highest probability for each particular plot (Table A-4). Compared with the observed reburn severity, the model achieved an overall accuracy rate of 76% (Table 3-6). According to the confusion matrix (Table 3-6), the model had correct estimations of reburn severity for 53 plots (i.e., principle diagonal elements, 76%), overestimated the reburn severity in 9 plots (i.e., upper diagonal elements, 13%), and underestimated the reburn severity in 8 plots (i.e., lower diagonal elements, 11%). A

Kappa statistic of 0.64 was achieved, implying substantial agreement between the predicted and observed reburn categories (Cohen 1960).

Table 3-5 Model parameters and corresponding p-values. Variables were identified as statistically significant (p-value ≤ 0.05) and as providing suggestive but inconclusive evidence in the model (0.05 < p-value ≤0.1) (Ramsey and Schafer 2013).

Variable	Estimated coefficient	Standard error	p-value
Relative change of live tree BA (a)	-3.759	1.3	0.004
Relative change of live small tree TPH (b)	0.850	1.1	0.45
Post-first fire live conifer BA	0.0556	0.03	0.09
Interaction between (a) and (b)	1.4658	0.7	0.04

Table 3-6 Confusion matrix to compare predicted and observed reburn severity. Elements in the confusion matrix represented the number of plots in each combination of predicted and observed reburn severity. Refer to Table 3-3 for details of the reburn severity definition.

		Predicted reburn severity				
		0	1	2	3	Total
Observed reburn severity	0	15	0	0	0	15
	1	4	27	8	0	39
	2	0	0	6	1	7
	3	0	2	2	5	9
	Total	19	29	16	6	70

3.4 Discussion

3.4.1 Different stand structure in two forest patch types

Fire behaviour and fire characteristics may differ among forest patch types due to differences in stand structure (Fernandes 2009); thus, pre-first fire structural differences in continuous and fragmented forest patches were examined. Before the occurrence of the first fire, plots in fragmented forest patches generally had lower live tree TPH and BA, regardless of tree species and size. The explanation of this finding is straightforward: plots in fragmented forest patches were located in a series of "forest islands" with patches of trees interspersed with grasslands, thus resulting in lower live tree TPH and BA. Further, both sites in fragmented forest patches (i.e., RC and RP) were dominated by lodgepole pine. Thus, live tree density decreased in both sites with the mountain pine beetle outbreak (from 1998 with a peak in 2004), the following salvage logging (in 2007 and 2008), and the grassland restoration (in 2008).

High variation in live aspen TPH and BA among plots was evident before the first fire, which reflected the heterogeneity in species composition within a site. For example for site MG, seven out of 20 plots were dominated by aspen trees (>225 TPH, >80% of BA), while 13 plots were dominated by conifer trees, where aspen trees were less dominant (<100 TPH, <30% of BA). This high variation of aspen trees among plots within a site may also explain the variation of the reburn severity among plots within a site. Specifically, plots that were dominated by aspen trees at site MG before the first fire (i.e., seven plots mentioned above) generally had lower reburn severity than other plots at the site. This observation aligned with a previous study showing that aspen stands were less likely to burn than other cover types in subalpine forests (Bigler et al. 2005).

High variation in dead tree TPH and BA among plots was also found before the first fire. Different amounts of dead trees in plots resulted from the mountain pine beetle outbreak, the following salvage logging, and the grassland restoration. Specifically, natural and anthropogenic disturbances caused heterogeneity in the number of dead trees, especially dead pines, among plots (Figure A-1).

3.4.2 Positive relationship between severities in successive forest fires

The final model achieved an overall accuracy of 76% and implied that greater relative change of live tree BA, a proxy for the severity of the first fire, was associated with higher reburn severity. One extreme case of the loss in live tree BA after the first fire was at site MG, where post-fire logging and replanting were conducted in nine plots (Figure 3-4, Figure A-2, Figure A-3). These logged and replanted plots severely burned during the reburn in 2017. Previous research has shown that post-fire logging could significantly increase downed woody fuels (Donato et al. 2006). Additionally, replanting activities after a post-fire logging could cause even higher severity given the vulnerability of seedlings to high severity reburns (Thompson et al. 2007). The observations from site MG suggest that post-fire logging with logging debris left on site and replanting potentially resulted in higher reburn severity at that given site. Note that in order to exclude the possibility of these nine plots confounding the modelling result, a new model was fit without those nine plots (results not presented). Variables as reported in Table 3-5 were still significant with slightly larger standard errors given a smaller number of observations, thus retaining the interpretation of the presented model.

Across all sites, the model result indicated that higher first fire severity was associated with higher reburn severity. This result aligns with previous research finding positive relationships between severities in successive fires in the Pacific Northwest (Thompson et al. 2007, Collins et al. 2009, van Wagtendonk et al. 2012). However, other research found an opposite relationship between reburn and first fire severity, where the first fire reduced the reburn severity (Teske et al. 2012, Larson et al. 2013, Parks et al. 2015, Harris and Taylor 2017, Lydersen et al. 2017). One explanation of this negative relationship is that the relationship between severities in successive fires is dependent on the fire return interval (Harvey et al. 2016). Specifically, fires can limit the spread and severity of the reburn up to 10 years post-fire; however, about 10 years after a fire, the reburn severity could potentially be equal or greater than that of the first fire (Harvey et al. 2016). In this study, the reburn occurred seven or eight years after the first fire, which is close to the previously estimated period of 10 years of limiting reburn severity (Harvey et al. 2016). It may be possible that the study sites were already past this limiting fire effect and thus exhibited a positive relationship between fire severities.

3.4.3 Longitudinal data: key for studying relationships between successive forest fires

One limitation of this study was the lack of pre-reburn measurement. Pre-fire forest structure information is crucial in modelling fire severity, as specified by Collins et al. (2018) who found that pre-fire live conifer tree BA was an important predictor of fire severity. In this study, the post-first fire measurement was the closest available data regarding the pre-reburn forest structure, but there was still a seven or eight year interval in between this measurement and the reburn. The measurement might thus not be representative for the pre-reburn stand structure given that fuel accumulation, snag decay, and delayed mortality of standing trees can alter the stand structure substantially within the first 10 years after fires (Foster et al. 2017).

In order to develop a database that captures fire disturbances temporally, a long-term monitoring program with spatially balanced plots and systematic remeasurements should be considered in BC. Specifically, in 2013, the Provincial Change Monitoring Inventory (CMI) program was initiated by BC government aiming to monitor changes at a broad, landscape scale and at regular time intervals (Province of BC 2018). Field measured data one year post-fire, as collected by the Fire Effects and Recovery Study in Untied States (Forest Inventory and Analysis 2017), can be added based on the current plots in order to evaluate the impacts of forest fire on forest condition. With a long-term monitoring program and detailed post-fire measurements, studies requiring longitudinal data, such as fuel dynamics after fires (Eskelson and Monleon 2018, Eskelson et al. 2016), could thus be possible in BC.

3.4.4 The use of satellite imagery in measuring fire severity

Previous research investigating relationships of severities in successive fires commonly used fire severity from Landsat satellite imagery, given its high accessibility and advantage in deriving pre-fire information that might be difficult to retrieve in the field (Morgan et al. 2014). Despite its convenience, Landsat-derived fire severity is not suitable in this study for several reasons. First, the spatial resolution of the Landsat imagery is not fine enough for the study plots. Specifically, the fire severity of a small circular plot in this study (radius of 11.3 meters) would be represented by a single pixel (30 meters resolution) of Landsat imagery. This might result in a low signal to noise ratio for the fire severity classification (Young et al. 2017). Second, Landsat-derived fire severity can be problematic when comparing its value across different forest types, such as in this study, given its nature in detecting the change in vegetation cover (Key and Benson 1999; Miller and Thode 2007).

3.4.5 Data science for drawing inferences

Models for drawing inferences were built in order to gain an understanding of how the explanatory variables drive the distribution of the response variable (Hawkins 2003). Statistical models have a great focus on the interpretability of a model, aiming to derive causal inference and inference to populations (Ramsey and Schafer 2013). Machine learning, on the other hand, finds the underlying patterns of data, with a strong emphasis on prediction but not suitable for building models for interpretation (Dhar 2012).

In this case study, three kinds of interpretation can be derived from the ordinal logistic model. First, the overall accuracy and Cox and Snell R^2 (Cox and Snell 1968) were used to indicate the goodness-of-fit of the model on the data. The goodness-of-fit indicators can provide an overall perception of how well the explanatory variables were explaining the distribution of the response variable. Second, the estimation power of each explanatory variable in the ordinal logistic model were defined by the significance level of the coefficients. The significance level enables a stepwise selection (i.e., forward selection), which keeps the explanatory variables most associated with the response (Hosmer et al. 2013). Finally, how each explanatory variable is associated with the response variable was interpreted through the value of the estimated coefficients (Hosmer et al. 2013).

3.5 Conclusions

British Columbia has experienced unprecedented fire seasons in recent years, with fires influencing human health, ecosystem services, environment, and biodiversity. Developing and applying innovative post-fire management strategies is crucial in order to lower the probability of reburn and, if reburn happens, lower the severity of the reburn. In general, this study found a positive relationship between severities in successive fires in the Riske Creek area of interior BC. Specifically, relative change of BA during the first fire was the most powerful explanatory variable of reburn severity. This positive relationship between relative change of BA and reburn severity indicated that fires might not be able to limit the probability or severity of a reburn after seven or eight years of a fire in the Riske Creek area. At one of the study sites, plots that were originally dominated by Douglas-fir before the first fire and experienced post-fire logging and replanting were severely burned compared to other plots at the same site that were originally dominated by aspen and did not receive post-fire management. The relationship between pre-fire aspen and reburn severity, and the relationship between post-fire management with reburn severity will need to be further investigated in future studies.

Chapter 4: Conclusion

4.1 Overall conclusions and future work

A bird sound detection model to predict bird presence in audio recordings was developed with frequency percentiles in a logistic model. This model can accurately predict the presence of bird sounds given an audio recording (i.e., 75% overall accuracy rate and 82% AUC), even with a large variability in the datasets. Further, the processing speed was over seven times faster than using the convolutional neural network (CNN) model, indicating the potential of this approach as a pre-filtering step within an overall bird identification algorithm. In particular, a pre-filtering step has potential to greatly reduce the time required to process audio recordings by eliminating the periods of recordings without bird sounds (Stowell et al. 2016). Future studies are needed to test this logistic detection on audio recordings collected from a smaller area with fewer species included in the audio recordings, where a better model performance is expected given decreased variation in the data.

For investigating the relationships between severities in successive forest fires, ordinal logistic models were developed to relate the forest stand structure metrics to the reburn severity in the Riske Creek area in interior British Columbia, Canada. In general, the model result indicated that higher first fire severity was associated with higher reburn severity. This result aligns with previous research finding positive relationships between severities in successive fires in the Pacific Northwest (Thompson et al. 2007, Collins et al. 2009, van Wagtendonk et al. 2012). This result indicates that previous fires have around a 6 to 7 year period that can limit the reburn severity and probability in the Riske Creek area. Finally, post-first fire logging and replanting might increase the reburn severity; while pre-fire aspen density might decrease the reburn severity. The relationship between aspen density and reburn severity was also found in a previous study showing that aspen stands were less likely to burn than other cover types (Bigler et al. 2005).

4.2 Limitations to the studies

The logistic detection model developed had some potential limitations. First, the detection model might not be useful for audio recordings collected during high sound activities, such as dawn recordings in bird abundant areas (e.g., boreal forests), where the majority of recording periods are with bird sounds and a pre-filtering step is not necessary. Second, the logistic detection model might miss the bird species with extreme low sound frequency (e.g., owl, grouse, ptarmigan), given that more high sound frequency percentiles were selected in the model. Further, the logistic detection model also got high false positive (35%) and false negative (16%) rates. For these false predictions, false positives would increase the examination effort after applying the detection model, but would not influence the truthfulness of the following analysis as the recordings of interest would be retained in the sample (Zwart et al. 2014). In contrast, false negatives would likely become an issue. The recordings were predicted to have bird absence, whereas they might include important information, particularly in the case that ‘filtered out’ recordings contain species of interest (Buxton and Jones 2012). This approach might still work if these 'filtered out' recordings do not include the target group of species being monitored.

One limitation of the fire study was the lack of pre-reburn measurements. Pre-fire forest structure information is crucial in modelling fire severity, as specified by Collins et al. (2018) who found that pre-fire live conifer tree BA was an important predictor of fire severity. In this study, the post-first fire measurement was the closest available data regarding the pre-reburn forest structure, but there was still a seven or eight year interval in between this measurement and the reburn. The measurement might thus not be representative for the pre-reburn stand structure given that fuel accumulation, snag decay, and delayed mortality of standing trees can alter the stand structure substantially within the first 10 years after fires (Foster et al. 2017).

4.3 Data science in action

This thesis contributes understanding of how machine learning modelling (innovative modelling) and statistical modelling (conventional modelling) could be applied in natural resources management. In the bird sound study, a predictive model was developed based on data across a large spatial scale; while in the fire severity study, an explanatory model was built to relate the previous fire severity to the reburn severity based on a relatively small set of data. Generality of the predictive model that was developed in the bird sound study can be achieved given the large spatial scale that the audio data covered. On the other hand, the explanatory model developed in the fire severity case study provided insights limited to the study area in the Riske Creek, British

Columbia. Even this, a case study like the fire severity study could be used to design future studies with larger spatial scale to discover the general pattern of fire severities across different ecosystems (Harvey et al. 2016).

Overall, this thesis demonstrates that both innovative (machine learning) and conventional (statistical) modelling have their own value, and that the selection of analysis tools depends on the research question to be answered, making prediction versus drawing inferences, and on the data structure, large scale versus small case study (Mannila 1996).

References

van der Aalst, W. 2016. Data science in action In: Process mining. *Springer, Berlin Heidelberg, Germany* 3–23.

Adavanne, S., K. Drossos, E. Cakir, and T. Virtanen. 2017. Stacked convolutional and recurrent neural networks for bird audio detection. *2017 25th European Signal Processing Conference (EUSIPCO), Kos island* 1729–1733.

Arts, K., R. van der Wal, and W. M. Adams. 2015. Digital technology and the conservation of nature. *Ambio* 44(S4): 661–673.

Ayer, T., J. Chhatwal, O. Alagoz, C. E. Kahn, R. W. Woods, and E. S. Burnside. 2010. Comparison of logistic regression and artifical neural network models in breast cancer risk estimation. *Informatics in Radiology* 30(1): 13–22.

BC Wildfire Service. 2017. Addressing the new normal: 21st century disaster management in British Columbia.

BC Wildfire Service. 2019. Wildfire season summary. [online] https://www2.gov.bc.ca/gov/content/safety/wildfire-status/about-bcws/wildfire-history/wildfire-season-summary. (Accessed on November 8 2019).

Bennet-Clark, H., and D. Young. 1994. The scaling of song frquency in cicadas. *Journal of Experimental Biology* 191(1): 291–294.

Bigler, C., D. Kulakowski, and T. T. Veblen. 2005. Multiple disturbance interactions and drought influence fire severity in Rocky Mountain subalpine forests. *Ecology* 86: 3018–3029.

Boll, S. 1979. Suppression of acoustic noise in speech using spectral subtraction. *IEEE Transactions on Acoustics, Speech, and Signal Processing* 27(2): 113–120.

Bonney, R. 2007. Citizen science at the Cornell Lab of Ornithology In: Exemplary science in informal education settings: standards-based success stories. *National Science Teachers Association, Virginia, USA.*

Brown, A., S. Garg, and J. Montgomery. 2019. Automatic rain and cicada chorus filtering of bird acoustic data. *Applied Soft Computing* 81: 105501.

Buxton, R. T., and I. L. Jones. 2012. Measuring nocturnal seabird activity and status using acoustic recording devices: applications for island restoration. *Journal of Field Ornithology* 83: 47–60.

Cakir, E., S. Adavanne, G. Parascandolo, K. Drossos, and T. Virtanen. 2017. Convolutional recurrent neural networks for bird audio detection. *2017 25th European Signal Processing Conference (EUSIPCO), Kos island* 1744–1748.

Cariboo-Chilcotin Grasslands Strategy Working Group. 2007. Cariboo-Chilcotin grasslands strategy.

Chollet, F. 2015. Keras. *Github repository*. [online] https://github.com/fchollet/keras (Accessed on November 8 2019).

Christensen, R. H. B. 2019. Ordinal: regression models for ordinal data. [online] http://www.cran.r-project.org/package=ordinal/ (Accessed on November 8 2019).

Cohen, J. 1960. A coefficient of agreement for nominal scales. *Educational and Psyschological Measurement* 1: 37–46.

Collins, B. M., J. D. Miller, A. E. Thode, M. Kelly, J. W. van Wagtendonk, and S. L. Stephens. 2009. Interactions among wildland fires in a long-established Sierra Nevada natural fire area. *Ecosystems* 12(1): 114–128.

Collins, B. M., J. M. Lydersen, R. G. Everett, and S. L. Stephens. 2018. How does forest recovery following moderate-severity fire influence effects of subsequent wildfire in mixed-conifer forests? *Fire Ecology* 14(2): 3.

Cox, D. R., and E. J. Snell. 1968. A general definition of residuals. *Journal of the Royal Statistical Society: Series B (Methodological)* 30(2): 248–265.

Daniels, L. D., Z. Gedalof, M. Pisaric, and K. A. Moser. 2013. Climate change, wildfire, and landscape homogenization in western Canada. *Research Update* 1–6.

Daniels, L. D., and R. W. Gray. 2006. Disturbance regimes in coastal British Columbia. *BC*

Journal of Ecosystem and Management 7(2): 44–56.

Daniels, L. D., R. W. Gray, B. Brett, P. D. Pickell, M. J. F. Pisaric, R. D. Chavardès, G. A. Greene, H. M. Marcous, and V. Comeau. 2017. Disturbance regimes in the Maritime to Submaritime forests of the south coast of British Columbia: status of knowledge and understanding. *BC Ministry of Forests, Lands and Natural Resource Operations*.

Daniels, L. D, R. W. Gray, and P. J. Burton. 2017. 2017 megafires in BC – urgent need to adapt and improve resilience to wildfire. [online] http://bccfa.ca/wp-content/uploads/2017/10/Lori-Daniels-2017-Wildfires-and-Resilience.pdf (Accessed on November 8 2019).

DeLong, E. R., D. M. DeLong, and D. L. Clarke-Pearson. 1988. Comparing the areas under two or more correlated receiver operating characteristic curves: a nonparametric approach. *Biometrics* 44(3): 837–845.

Dhar, V. 2012. Data science and prediction. *NYU Working Paper*.

Donato, D. C., J. B. Fontaine, J. L. Campbell, W. D. Robinson, J. B. Kauffman, and B. E. Law. 2006. Post-wildfire logging hinders regeneration and increases fire risk. *Science* 311(5759): 352.

Drake, K. L., M. Frey, D. Hogan, and R. Hedley. 2016. Using digital recordings and sonogram analysis to obtain counts of Yellow Rails. *Wildlife Society Bulletin* 40(2): 346–354.

Dreiseitl, S., and L. Ohno-Machado. 2002. Logistic regression and artificial neural network classification models: a methodology review. *Journal of Biomedical Informatics* 35(5–6): 352–359.

Drever, M. C., J. R. Goheen, and K. Martin. 2009. Species-energy theory, pulsed resources, and regulation of avian richness during a mountain pine beetle outbreak. *Ecology* 90(4): 1095–1105.

Dunn, C. J., and J. D. Bailey. 2015. Temporal fuel dynamics following high-severity fire in dry mixed conifer forests of the eastern Cascades, Oregon, USA. *International Journal of Wildland Fire* 24(4): 470.

Edworthy, A. B., and K. Martin. 2013. Persistence of tree cavities used by cavity-nesting vertebrates declines in harvested. *The Journal of Wildlife Management* 77(4): 770–76.

Eskelson, B. N. I., and V. J. Monleon. 2018. Post-fire surface fuel dynamics in California forests across three burn severity classes. *International Journal of Wildland Fire* 27(2): 114.

Eskelson, B. N.I., V. J. Monleon, and J. S. Fried. 2016. A 6 year longitudinal study of post-fire woody carbon dynamics in California's forests. *Canadian Journal of Forest Research* 46(5): 610–620.

Fernandes, P. M. 2009. Combining forest structure data and fuel modelling to classify fire hazard in Portugal. *Annals of Forest Science* 66(4): 415.

Forest Inventory and Analysis. 2017. Field instructions for the annual inventory of California, Oregon, and Washington. Supplement for: fire effects and recovery study. *Pacific Northwest research station.*

Foster, C. N., P. S. Barton, N. M. Robinson, C. I. MagGregor, and D. B. Lindenmayer. 2017. Effects of a large wildfire on vegetation structure in a variable fire mosaic. *Ecological Applications* 27(8): 2369–2381.

Garnett, S., J. Szabo, and G. Dutson. 2011. The action plan for Australian birds 2010. *CSIRO Publishing, Victoria, Australia.*

Geron, A. 2017. Hands-on machine learning with Scikit-Learn and Tensorflow: concepts, tools and techniques to build intelligient systems. *O'Reilly, Sebastopol, USA.*

Hafner, S, and J. Katz. 2017. MonitoR: acoustic template detection in R. [online] https://cran.r-project.org/web/packages/monitoR/index.html (Accessed on November 8 2019).

Harris, L., and A. H. Taylor. 2017. Previous burns and topography limit and reinforce fire severity in a large wildfire. *Ecosphere* 8(11): e02019.

Harvey, B. J., D. C. Donato, and M. G. Turner. 2016. Burn me twice, shame on who? Interactions between successive forest fires across a temperate mountain region. *Ecology* 97(9): 2272–2282.

Hawkins, D. M. 2003. The problem of overfitting. *Journal of Chemical Information and Modeling* 44(1): 1-12.

Hedley, R. W., Y.-W. Huang, and K. Yao. 2017. Direction-of-arrival estimation of animal vocalizations for monitoring animal behavior and improving estimates of abundance. *Avian Conservation and Ecology* 12(1): art6.

Heyerdahl, E. K., K. Lertzman, and C. M. Wong. 2012. Mixed-severity fire regimes in dry forests of southern interior British Columbia, Canada. *Canadian Journal of Forest Research* 42(1): 88–98.

Hosmer, D. W., S. Lemeshow, and R. X. Sturdivant. 2013. Applied Logistic Regression. *Wiley, New Jersey, USA.*

Jain, T. B., D. S. Pilliod, R. T. Graham, L. B. Lentile, and J. E. Sandquist. 2012. Index for characterizing post-fire soil environments in temperate coniferous forests. *Forests* 3(3): 445–466.

Joly, A., H. Goëau, C. Botella, S. Kahl, M. Servajean, H. Glotin, P. Bonnet, R. Planqué, F. Robert-Stöter, W.-P. Vellinga, and H. Müller. 2019. Overview of LifeCLEF 2019: identification of Amazonian plants, South & North American birds, and biche prediction. *Springer, Cham* 387–401.

Key, C. H., and N. C. Benson. 1999. The normalized burn ratio (NBR): a Landsat TM radiometric measure of burn severity. *United States Geological Survey, Northern Rocky Mountain Science Center.*

Kingma, D. P., and J. Ba. 2014. Adam: a method for stochastic optimization. *arXiv preprint* arXiv: 1462.6908.

Klingbeil, B. T., and M. R. Willig. 2015. Bird biodiversity assessments in temperate forest: the value of point count versus acoustic monitoring protocols. *PeerJ* 3: e973.

Knight, E. C., K. C. Hannah, G. J. Foley, C. D. Scott, R. M. Brigham, and E. Bayne. 2017. Recommendations for acoustic recognizer performance assessment with application to five common automated signal recognition programs. *Avian Conservation and Ecology* 12(2): art14.

Kong, Q., Y. Xu, and M. D. Plumbley. 2017. Joint detection and classification convolutional neural network on weakly labelled bird audio detection. *2017 25th European Signal Processing Conference (EUSIPCO), Kos island* 1749–1753.

Lambert, K. T. A., and P. G. McDonald. 2014. A low-cost, yet simple and highly repeatable system for acoustically surveying cryptic species. *Austral Ecology* 39(7): 779–785.

Larson, A. J., R. T. Belote, C. A. Cansler, S. A. Parks, and M. S. Dietz. 2013. Latent resilience in ponderosa pine forest: effects of resumed frequent fire. *Ecological Applications* 23(6): 1243–1249.

Levene, H. 1960. Robust tests for equality of variances. Contributions to Probability and Statistics. *Stanford University Press, Santa Clara County, USA.*

Lima, F. 2018. Convolutional neural networks in R. [online] https://www.r-bloggers.com/convolutional-neural-networks-in-r/ (Accessed on November 8 2019).

Lydersen, J. M., B. M. Collins, M. L. Brooks, J. R. Matchett, K. L. Shive, N. A. Povak, V. R. Kane, and D. F. Smith. 2017. Evidence of fuels management and fire weather influencing fire severity in an extreme fire event. *Ecological Applications* 27(7): 2013–2030.

Mannila, H. 1996. Data mining: machine learning, statistics, and databases. *8th International Conference on Scientific and Statistical Data Base Management.*

Marcoux, H. M., L. D. Daniels, S. E. Gergel, E. Da-Silva, Z. Gedalof, and P. F. Hessburg. 2015. Differentiating mixed- and high-severity fire regimes in mixed-conifer forests of the Canadian Cordillera. *Forest Ecology and Management* 341: 45–58.

Martin, K., and J. M. Eadie. 1999. Nest webs: a community-wide approach to the management and conservation of cavity-nesting forest birds. *Forest Ecology and Management* 115(2): 243–257.

Martin, K., K. E. H. Aitken, and K. L. Wiebe. 2004. Nest sites and nest webs for cavity-nesting communities in interior British Columbia, Canada: nest characteristics and niche partitioning. *The Condor* 106(1): 5–19.

McCullagh, P. 1980. Regression models for ordinal data. *Journal of the Royal Statistical Society: Series B (Methodological)* 42(2): 109–127.

McCullagh, P., and J. A. Nelder. 1989. Generalized linear models. *Routledge, London, United Kingdom*.

Meidinger, D., and J. Pojar. 1991. Ecosystems of British Columbia. *BC Ministry of Forests, Lands and Natural Resource Operations*.

Miller, J. D., and A. E. Thode. 2007. Quantifying burn severity in a heterogeneous landscape with a relative version of the delta normalized burn ratio (dNBR). *Remote Sensing of Environment* 109(1): 66–80.

Mladenoff, D. J., T. A. Sickley, and A. P. Wydeven. 1999. Predicting gray wolf landscape recolonization: logistic regression models vs. new field data. *Ecological Applications* 9(1): 37–44.

Morgan, P., R. E. Keane, G. K. Dillon, T. B. Jain, A. T. Hudak, E. C. Karau, P. G. Sikkink, Z. A. Holden, and E. K. Strand.. 2014. Challenges of assessing fire and burn severity using field measures, remote sensing and modelling. *International Journal of Wildland Fire* 23(8): 1045.

Neter, J, M. H. Kutner, C. J. Nachtsheim, and W. Wasserman. 1996. Applied linear statistical models. *McGraw-Hill/Irwin, New York, USA.*

O'Connell, A. F., J. D. Nichols, and K. U. Karanth. 2011. Camera traps in animal ecology: methods and analyses. *Springer, New York, USA.*

de Oliveira, A. G., T. M. Ventura, T. D. Ganchev, J. M. de Figueiredo, O. Jahn, M. I. Marques, and K.-L. Schuchmann. 2015. Bird acoustic activity detection based on morphological filtering of the spectrogram. *Applied Acoustics* 98: 34–42.

Parks, S. A., L. M. Holsinger, C. Miller, and C. R. Nelson. 2015. Wildland fire as a self-regulating mechanism: the role of previous burns and weather in limiting fire progression. *Ecological Applications* 25(6): 1478–1492.

Pearce, J., and S. Ferrier. 2000. Evaluating the predictive performance of habitat models developed using logistic regression. *Ecological Modelling* 133(3): 225–245.

Pellegrini, T. 2017. Densely connected CNNs for bird audio detection. *2017 25th European Signal Processing Conference (EUSIPCO), Kos island* 1734–1738.

Pieretti, N., A. Farina, and D. Morri. 2011. A new methodology to infer the singing activity of an avian community: the acoustic complexity index (ACI). *Ecological Indicators* 11(3): 868–

873.

Pimm, S. L., S. Alibhai, R. Bergl, A. Dehgan, C. Giri, Z. Jewell, L. Joppa, R. Kays, and S. Loarie. 2015. Emerging technologies to conserve biodiversity. *Trends in Ecology & Evolution* 30(11): 685–696.

Procaccini, A., A. Orlandi, A. Cavagna, I. Giardina, F. Zoratto, D. Santucci, F. Chiarotti, C. K. Hemelrijk, E. Alleva, G. Parisi, and C. Carere. 2011. Propagating waves in starling, sturnus vulgaris, flocks under predation. *Animal Behaviour* 82(4): 759–765.

Province of BC. 1995. Biodiversity guidebook. *Canadian Cataloguing in Publication Data and BC Environment, Victoria, Canada.*

Province of BC. 2018. Provincial change monitoring inventory (CMI) and young stand monitoring (YSM) sampling framework. *BC Ministry of Forests, Lands and Natural Resource Operations*.

R Core Team. 2019. R: a language and environment for statistical computing.

Ramsey, F. L., and D. W. Schafer. 2013. The statistical sleuth: a course in methods of data analysis. *Cengage Learning, Boston, USA.*

Rognan, C. B., J. M. Szewczak, and M. L. Morrison. Autonomous recording of Great Gray Owls in the Sierra Nevada. *Northewstern Naturalist* 93(2): 138–144.

Rosenstock, S. S., D. R. Anderson, K. M. Giesen, T. Leukering, and M. F. Carter. 2002. Landbird counting techniques: current practices and an alternative *The Auk* 119(1): 46–53.

Rumsey, F., and T. Mccormick. 2012. Sound and recording. *Routledge, Abingdon, United Kingdom.*

Schaffer, C. 1993. Overfitting avoidance as bias. *Machine Learning* 10(2): 153–178.

Schrama, T., M. Poot, M. Robb, and H. Slabbekoorn. 2007. Automated monitoring of avian flight calls during nocturnal migration. *International Expert Meeting on IT-Based Detection of Bioacoustical Patterns*.

Shonfield, J., and E. M. Bayne. 2017. Autonomous recording units in avian ecological research:

current use and future applications. *Avian Conservation and Ecology* 12(1): art14.

Simons, T. R., M. W. Alldredge, K. H. Pollock, and J. M. Wettroth. 2007. Experimental analysis of the auditory detection process on avian point counts. *The Auk* 124(3): 986–999.

Snee, R. D. 1977. Validation of regression models: methods and examples. *Technometrics* 19(4): 415–428.

Song, M.-L., R. Fisher, J.-L. Wang, and L.-B. Cui. 2018. Environmental performance evaluation with big data: theories and methods. *Annals of Operations Research* 270(1–2): 459–472.

Sovern, S. G., E. D. Forsman, G. S. Olson, B. L. Biswell, M. Taylor, and R. G. Anthony. 2014. Barred owls and landscape attributes influence territory occupancy of Northern Spotted Owls. *The Journal of Wildlife Management* 78(8): 1436–1443.

Srivastava, N., G. Hinton, A. Krizhevsky, I. Sutskever, and R. Salakhutdinov. 2014. Dropout: a simple way to prevent neural networks from overfitting. *Journal of Machine Learning Research* 15: 1929–1958.

Stowell, D., and M. D. Plumbley. 2014. An open dataset for research on audio field recording archives: Freefield1010. *53rd International Conference, Semantic Audio, London, United Kingdom.*

Stowell, D., M. Wood, Y. Stylianou, and H. Glotin. 2016. Bird detection in audio: a survey and a challenge. *2016 IEEE 26th International Workshop on Machine Learning for Signal Processing (MLSP).*

Student. 1908. The probable error of a mean. *Biometrika* 6(1): 1.

Sueur, J., A. Farina, A. Gasc, N. Pieretti, and S. Pavoine. 2014. Acoustic indices for biodiversity assessment and landscape investigation. *Acta Acustica united with Acustica* 100(4): 772–781.

Sueur, J., S. Pavoine, O. Hamerlynck, and S. Duvail. 2008. Rapid acoustic survey for biodiversity appraisal. *PLoS ONE* 3(12): e4065.

Sun, Z.-Y., and H. Ren. 2011. Ecological memory and its potential applications in ecology: a review. *The journal of applied ecology* 22(3): 549–555.

Tabachnick, B. G., and L. S. Fidell. 2019. Using multivariate statistics. *Pearson Education, London, United Kingdom.*

Tabak, M. A., M. S. Norouzzadeh, D. W. Wolfson, S. J. Sweeney, K. C. Vercauteren, N. P. Snow, J. M. Halseth, P. A. Di-Salvo, J. S. Lewis, M. D. White, B. Teton, J. C. Beasley, P. E. Schlichting, R. K. Boughton, B. Wight, E. S. Newkirk, J. S. Ivan, E. A. Odell, R. K. Brook, P. M. Lukacs, A. K. Moeller, E. G. Mandeville, J. Clune, and R. S. Miller. 2019. Machine learning to classify animal species in camera trap images: applications in ecology *Methods in Ecology and Evolution* 10(4): 585–590.

Tanttu, J. T., J. Turunen, A. Selin, and M. Ojanen. 2006. Automatic feature extraction and classification of crossbill (*loxia spp.*) flight calls. *Bioacoustics* 15(3): 251–269.

Tchernichovski, O., F. Nottebohm, C. E. Ho, B. Pesaran, and P. P. Mitra. 2000. A procedure for an automated measurement of song similarity. *Animal Behaviour* 59(6): 1167–1176.

Teske, C. C., C. A. Seielstad, and L. P. Queen. 2012. Characterizing fire-on-fire interactions in three large wilderness areas. *Fire Ecology* 8(2): 82–106.

Thompson, J. R., T. A. Spies, and L. M. Ganio. 2007. Reburn severity in managed and unmanaged vegetation in a large wildfire. *Proceedings of the National Academy of Sciences of the United States of America* 104(25): 10743–48.

Towsey, M. W. 2013. Noise removal from wave-forms and spectrograms derived from natural recordings of the environment.

Towsey, M., J. Wimmer, I. Williamson, and P. Roe. 2014. The use of acoustic indices to determine avian species richness in audio-recordings of the environment. *Ecological Informatics* 21: 110–119.

Upton, E., M. Veloso, A. Gadgil, T. White, B. Monks, and R. Malkin. 2015. Today’s engineering heroes. *IEEE Spectrum* 52(3): 39–49.

van Wagtendonk, J. W., K. A. van Wagtendonk, and A. E. Thode. 2012. Factors associated with the severity of intersecting fires in Yosemite National Park, California, USA. *Fire Ecology* 7(1): 11–31.

Warblr. 2015. Warblr: identify UK bird songs and calls. [online] https://www.warblr.co.uk/

(Accessed on November 8 2019).

Wolfe, R., and W. Gould. 1998. An approximate likelihood-ratio test for ordinal response models. *Stata Technical Bulletin* 7(42): 24–27.

Young, N. E., R. S. Anderson, S. M. Chignell, A. G. Vorster, R. Lawrence, and P. H. Evangelista. 2017. A survival guide to landsat preprocessing. *Ecology* 98(4): 920–932.

Zwart, M. C., A. Baker, P. J. K. Mcgowan, and M. J. Whittingham. 2014. The use of automated bioacoustic recorders to replace human wildlife surveys: an example using nightjars. *Plos One* 9(7): e102770.

Appendix: Additional figures and tables for Chapter 3

Table A-1 Basal area per hectare, species composition, tree density, and DBH distribution by site in 1998.

Abbreviations: DBH: diameter at the breast height; SD: standard deviation.

	Site				
	MG	RC	RL	RP	SW
Total basal area per hectare (m^2ha^{-1})	545	134	265	214	215
Species composition by basal area (%)					
Trembling Aspen	13	31	3	6	14
Lodgepole Pine	13	63	42	74	13
Douglas-fir	74	6	49	21	73
Spruce sp.	0	0	6	0	0
Tree density (trees ha^{-1})					
Trembling Aspen	121	91	12	42	53
Lodgepole Pine	83	234	232	323	85
Douglas-fir	344	16	160	19	192
Spruce sp.	0	0	27	0	0
DBH (cm)					
Mean	22.2	23.6	21.5	21.7	21.8
SD	11.9	8.38	7.85	11.0	8.83
max	88.3	51.5	57.5	105.0	68.4

Table A-2 Basal area per hectare, species composition, tree density, and DBH distribution by sites post first fire. Post first fire: 2010 measurement for RC, RL, RP and 2011 for MG, SW. Abbreviation: DBH: diameter at the breast height; SD: standard deviation.

	Site				
	MG	RC	RL	RP	SW
Total basal area per hectare (m^2ha^{-1})	213	92	216	149	191
Species composition by basal area (%)					
Trembling Aspen	44	40	4	14	9
Lodgepole Pine	5	49	26	53	5
Douglas-fir	51	11	63	33	86
Juniper sp.	0	0	0	0	0
Spruce sp.	0	0	7	0	0
Tree density (trees ha^{-1})					
Trembling Aspen	189	103	10	92	48
Lodgepole Pine	15	150	93	177	38
Douglas-fir	98	31	172	35	193
Juniper sp.	3	0	0	0	0
Spruce sp.	0	0	27	0	0
DBH (cm)					
Mean	19.5	21.4	23.1	19.6	21.8
SD	8.42	7.57	8.61	11.7	10.1
max	74.9	45.5	57.5	105.0	68.4

Table A-3 Basal area per hectare, species composition, tree density, and DBH distribution by sites post-reburn (2018). Abbreviation: DBH: diameter at the breast height; SD: standard deviation.

	Site				
	MG	RC	RL	RP	SW
Total basal area per hectare (m^2ha^{-1})	127	52	235	91	86
Species composition by basal area (%)					
Trembling Aspen	65	69	2	40	11
Lodgepole Pine	0	13	2	27	2
Douglas-fir	34	18	86	33	87
Juniper sp.	1	0	0	0	0
Spruce sp.	0	0	10	0	0
Tree density (trees ha^{-1})					
Trembling Aspen	173	122	7	115	23
Lodgepole Pine	0	19	10	46	7
Douglas-fir	36	12.5	172	35	30
Juniper sp.	1	0	0	0	0
Spruce sp.	0	0	32	0	0
DBH (cm)					
Mean	18.4	21.1	27.6	20.3	30.8
SD	6.95	9.97	11.8	9.01	16.6
max	57.7	44.9	69.6	75.4	70.7

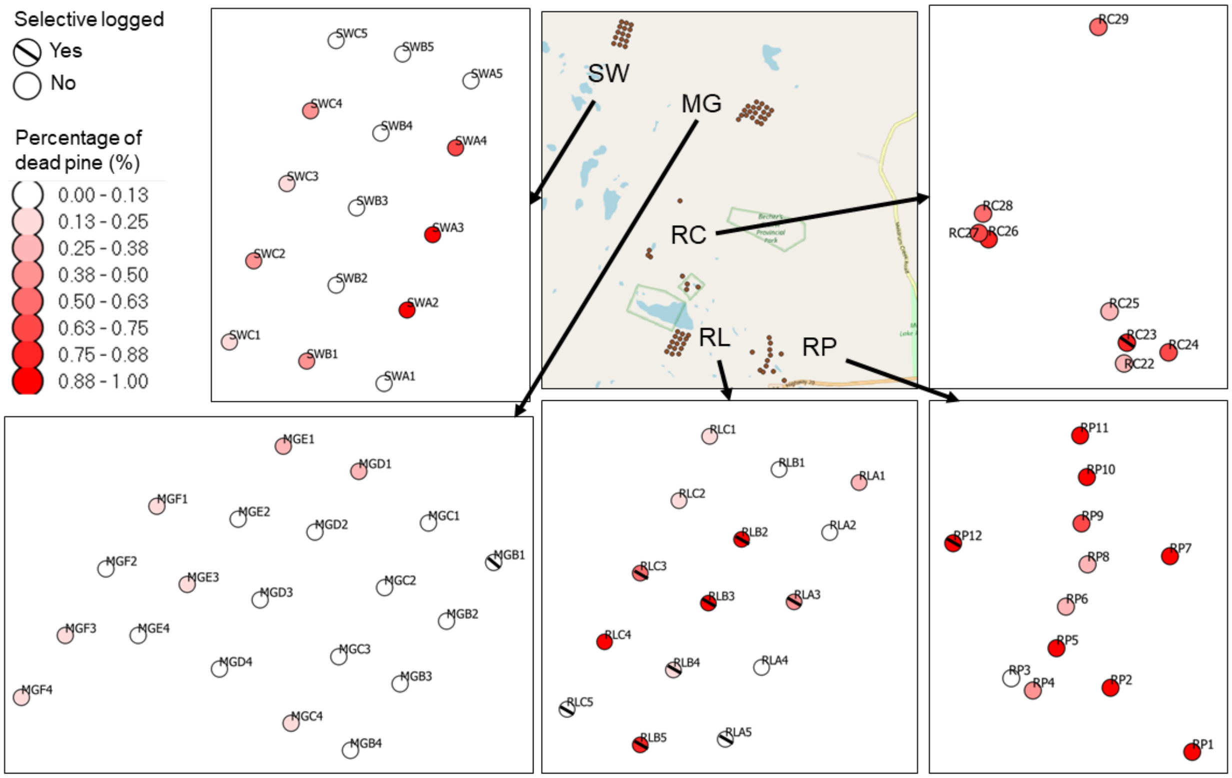

Figure A-1 Percentage of dead pines in each plot before the first fire. Salvage logging occurred in some of the plots in 2007 and 2008.

Table A-4 Predicted probabilities (P) for each reburn severity categories, predicted reburn severity category, and observed reburn severity category.

Plot	P(reburn severity=0)	P(reburn severity=1)	P(reburn severity=2)	P(reburn severity=3)	Predicted reburn severity	Observed reburn severity
MGB1	0.1	0.73	0.16	0.01	1	1
MGB2	0.08	0.71	0.2	0.01	1	1
MGB3	0	0.06	0.47	0.48	3	3
MGB4	0.02	0.47	0.46	0.05	1	2
MGC1	0.1	0.73	0.16	0.01	1	1
MGC2	0.01	0.24	0.61	0.14	2	3
MGC3	0	0.06	0.47	0.48	3	3
MGC4	0.01	0.2	0.62	0.18	2	2
MGD1	0.08	0.71	0.19	0.01	1	1
MGD2	0.09	0.72	0.18	0.01	1	1
MGD3	0	0.06	0.47	0.48	3	3
MGD4	0	0.06	0.47	0.48	3	3
MGE1	0.04	0.6	0.33	0.03	1	1
MGE2	0	0.06	0.47	0.48	3	1
MGE3	0	0.06	0.47	0.48	3	2
MGE4	0	0.15	0.61	0.24	2	2
MGF1	0.08	0.71	0.2	0.01	1	1
MGF2	0	0.06	0.47	0.48	3	3
MGF3	0	0.06	0.47	0.48	3	2
MGF4	0	0.06	0.47	0.48	3	1
RC22	0.05	0.66	0.27	0.02	1	2
RC23	0.01	0.21	0.62	0.16	2	2
RC24	0.03	0.56	0.37	0.04	1	2
RC25	0.05	0.64	0.29	0.02	1	1
RC26	0.22	0.7	0.07	0	1	1
RC27	0.09	0.72	0.17	0.01	1	2
RC28	0.1	0.73	0.17	0.01	1	0
RC29	0.09	0.72	0.17	0.01	1	0
RLA1	0.05	0.65	0.27	0.02	1	1

Plot	P(reburn severity=0)	P(reburn severity=1)	P(reburn severity=2)	P(reburn severity=3)	Predicted reburn severity	Observed reburn severity
RLA2	0.03	0.51	0.42	0.04	1	1
RLA3	0.13	0.74	0.12	0.01	1	1
RLA4	0.15	0.73	0.11	0.01	1	1
RLA5	0.15	0.73	0.11	0.01	1	1
RLB1	0.01	0.3	0.58	0.11	2	2
RLB2	0.15	0.73	0.11	0.01	1	1
RLB3	0.15	0.73	0.11	0.01	1	1
RLB4	0.12	0.73	0.14	0.01	1	2
RLB5	0.14	0.73	0.11	0.01	1	1
RLC1	0.04	0.6	0.33	0.03	1	1
RLC2	0.11	0.73	0.15	0.01	1	1
RLC3	0.12	0.73	0.13	0.01	1	1
RLC4	0.14	0.73	0.12	0.01	1	1
RLC5	0.12	0.73	0.14	0.01	1	1
RP1	0.13	0.74	0.13	0.01	1	0
RP2	0.02	0.49	0.44	0.05	1	2
RP3	0.13	0.74	0.12	0.01	1	2
RP4	0	0.16	0.62	0.22	2	2
RP5	0.13	0.74	0.13	0.01	1	2
RP6	0.22	0.71	0.07	0	1	0
RP7	0.13	0.74	0.13	0.01	1	1
RP8	0.13	0.74	0.13	0.01	1	1
RP9	0.13	0.74	0.13	0.01	1	1
RP10	0	0.07	0.52	0.4	2	2
RP11	0.13	0.74	0.13	0.01	1	1
RP12	0.13	0.74	0.13	0.01	1	1
SWA1	0.95	0.05	0	0	0	0
SWA2	1	0	0	0	0	0
SWA3	1	0	0	0	0	0
SWA4	0.73	0.26	0.01	0	0	0
SWA5	0.97	0.03	0	0	0	0
SWB1	0.99	0.01	0	0	0	0
SWB2	0.99	0.01	0	0	0	0

Plot	P(reburn severity=0)	P(reburn severity=1)	P(reburn severity=2)	P(reburn severity=3)	Predicted reburn severity	Observed reburn severity
SWB3	0.99	0.01	0	0	0	0
SWB4	0.99	0.01	0	0	0	0
SWB5	0.89	0.1	0	0	0	0
SWC1	0.99	0.01	0	0	0	0
SWC2	0.98	0.02	0	0	0	0
SWC3	0.99	0.01	0	0	0	0
SWC4	1	0	0	0	0	0
SWC5	0.99	0.01	0	0	0	0

Figure A-2 Post-fire logging in 2011 left large size logging debris on site, which might result in the severe reburn in 2017. Photo taken by Yi-Chin Tseng for plot MGB3 in 2018 June.

Figure A-3 Post-fire logging in 2011 left large size logging debris on site, which might result in the severe reburn in 2017. Photo taken by Yi-Chin Tseng for plot MGB4 in 2018 June.